OUKA
The University of Osaka
Institutional Knowledge Archive

Title	Solution Properties of Polymacromonomers Consisting of Polystyrene
Author(s)	Terao, Ken
Citation	大阪大学, 1999, 博士論文
Version Type	VoR
URL	https://doi.org/10.11501/3155179
rights	
Note	

The University of Osaka Institutional Knowledge Archive : OUKA

https://ir.library.osaka-u.ac.jp/

The University of Osaka

甲6695

Solution Properties of Polymacromonomers Consisting of Polystyrene

A Doctoral Thesis

by

Ken Terao

Submitted to

the Graduate School of Science, Osaka University

February, 1999

Solution Properties of Polymacromonomers Consisting of Polystyrene

A Doctoral Thesis

by

Ken Terao

Submitted to

the Graduate School of Science, Osaka University

February, 1999

APPROVALS

February, 1999

This thesis is approved as to the style and content by

則末尚志

Member-in-chief

足立桂一郎

Member

Member

佐藤尚弘

Member

Acknowledgment

This thesis work was performed from 1996 to 1999 under the direction of Professor Takashi Norisuye at the Department of Macromolecular Science, Graduate School of Science, Osaka University. I thank Professor Takashi Norisuye and Dr. Yo Nakamura for their guidance, advice, and encouragement throughout the course of this work.

I also wish to extend my sincere appreciation to Professor Emeritus Akio Teramoto, Associate Professor Takahiro Sato, and Dr. Yuji Jinbo for their helpful advice and valuable discussions. I am very grateful to Professor Jimmy W. Mays of the University of Alabama at Birmingham for his help in MALDI-TOF-mass spectroscopy. Thanks are due to Mr. Yoshishige Takeo and Mr. Masataka Tazaki for offering a polystyrene macromonomer sample, and Mr. Toshio Hokajo and Ms. Setsuyo Hayashi for helping me with fractionation and viscometry. Thanks are extended to all the members of Norisuye's laboratory for their encouragement and friendship.

Finally I would like to thank my parents Tsuyoshi and Motoko Terao for their constant encouragement.

寺尾 憲

Ken Terao

Toyonaka, Osaka

February, 1999

Contents

Chapter I General Introduction

I. 1 Purposes of This Work

Systematic experimental work done on dilute polymer solutions in the past two decades has shown that dimensional and hydrodynamic properties of unperturbed linear polymer chains, either flexible or stiff, are explained almost quantitatively on the basis of the Kratky-Porod wormlike chain[1] or Yamakawa's more general model[2] called the helical wormlike (HW) chain. Although the former model is included by the latter one as a special case and fails to mimic the behavior of flexible chains with irregular helical conformations, it is applicable to a variety of semiflexible polymers[3] including regular helices with or without flexibility, and allows experimental determination of the chain stiffness and the contour length or helix pitch per main-chain residue for those polymers. Here, the chain stiffness in the wormlike chain model is specified by the persistence length q or the Kuhn segment length λ^{-1} (= $2q$) which is equal to the static stiffness parameter in the wormlike chain limit of the HW model.

Another important progress made in dilute-solution studies is the construction of the quasi-two-parameter (QTP) theory[2,4,5] (or the Yamakawa-Stockmayer-Shimada theory) based on the wormlike or HW chain. Well-documented experimental studies have indeed shown that this theory, an extension of the classical two-parameter theory[6] for long flexible chains, is capable of almost quantitatively describing intramolecular excluded-volume

effects in linear flexible and semiflexible polymers.[2,7-12] Thus the current theories for the HW model allows a unified description of dilute solutions of (uncharged) linear chains covering the entire range of conformation from coil to rod.

On the other hand, our understanding of branched polymer solutions is still far below the level that has been reached for linear polymers. There is no general way of determining the degree of branching or the structure of an irregularly branched polymer from dilute-solution measurements even in the unperturbed state. Efforts have thus been made to synthesize regular-branched polymers and explore their dilute solutions in the hope of elucidating the relationship between the molecular architecture and solution properties. A typical example is star polymers, which are the simplest in that they have only one branched point per molecule and the well-defined number of branches (arms) with a uniform length.

Solution studies now available in the literature[13,14] show that measured z-average mean-square radii of gyration $\langle S^2 \rangle_z$ of such polymers having sufficiently long arms in Θ solvents agree well with the theoretical prediction[15] for Gaussian stars if the arm number is less than 10. Semi-quantitative agreements between theory[16,17] and experiment[13,14] are also found for the arm number dependence of the hydrodynamic radius and the intrinsic viscosity $[\eta]$ in the Θ state. Though not quite satisfactory, these findings give us an insight into effects of long branches on solution properties. We note, however, that excluded-volume effects in star chains still leave much to be desired and that their detailed analyses have only recently been made for

four-arm star polystyrene (PS) by Okumoto et al.[18,19]

Comb-shaped polymers with uniform side chain lengths are another class of regular-branched chains. Noda et al.,[20] investigating cyclohexane solutions of such polystyrenes having different degrees of branching by light scattering and viscometry, found that the second virial coefficient A_2 vanishes at 31 – 33°C (near the Θ temperature 34.5°C for linear PS[21]) and that $\langle S^2 \rangle_z$ at the Θ point becomes appreciably larger than predicted for Gaussian combs[22] as the number of branches increases. These workers[20] suspected that an increase in segment density around branched points causes the PS chain to expand or extend even in the Θ state. Until recently, however, not much attention has been paid on this important suggestion, because the samples studied were heterogeneous with respect to branching point distribution and hence not desirable for use in a quantitative analysis.

The latest progress in the synthesis of regular-branched polymers made it possible to obtain fully regular combs by polymerizing nearly monodisperse macromonomers. Tsukahara et al.[23-25] were the first to synthesize polymacromonomers consisting of the poly(methyl methacrylate) (PMMA) backbone and PS side chains shown in Figure I-1, in which N and n denote the degrees of polymerization of the main chain and each side chain, respectively. This type of comb polymer is of great interest since it has features that (1) all side chains have almost equal lengths, (2) branching regularly occurs along the main chain, and (3) the monomer density is very high around the main chain. In fact, the polymacromonomers synthesized by Tsukahara et al.[23-25] called considerable attention of polymer physical chemists[26-28] who are interested in

molecular characterization of polymers in dilute solution.

Wintermantel et al.[26,27] and Nemoto et al.[28] analyzed dimensional and hydrodynamic data for these polymacromonomers in toluene, a good solvent, on the basis of the unperturbed wormlike chain to find that the regular comb polymers studied are much stiffer than linear PMMA and that λ^{-1} becomes larger as the molecular weight of the PS side chain increases. This pronounced effect of branching on chain stiffness raises a new matter of interest to be explained in terms of interactions between neighboring side chains in a polymer molecule. For fundamental studies of such intramolecular interactions, however, use of polymacromonomers composed of single polymer species is desirable to avoid complexity arising from interactions between the PMMA and PS sub-chains. Furthermore, Wintermantel et al.[26] encountered a problem that the unperturbed wormlike chain model did not always give a consistent explanation of measured $\langle S^2 \rangle_z$ and $[\eta]$ in toluene. This finding is serious, since, if literally taken, it indicates need of a new stiff-chain model for explaining dilute-solution behavior of polymacromonomers.

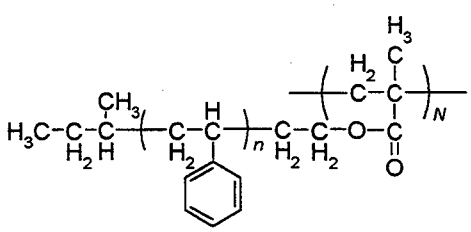

Figure I-1. Chemical structure of a polymacromonomer consisting of the PMMA backbone and PS side chains.

The present thesis is concerned with light scattering and viscometric studies on polymacromonomers consisting only of PS, whose chemical structure is shown in Figure I-2. Tsukahara et al.[29] already synthesized polymers of this kind but reported no solution data. As mentioned above, solution studies on polymacromonomers are yet limited to a few and not detailed enough to understand conformational features of the polymers in relation to the molecular characteristics of the linear chains composing them. In this work, we therefore collect data of $\langle S^2 \rangle_z$ and $[\eta]$ for our polymacromonomers covering a broad range of main chain length in cyclohexane and toluene (see Section I. 2) and check the applicability of the wormlike chain model or attempt to explain those data in a consistent way. We then examine the effects of side chain length and monomer – monomer interactions on the polymacromonomer conformation or structure, hoping that the present analysis serves for a deeper understanding of the relationship between the molecular architecture and solution properties of comb polymers or highly branched polymers.

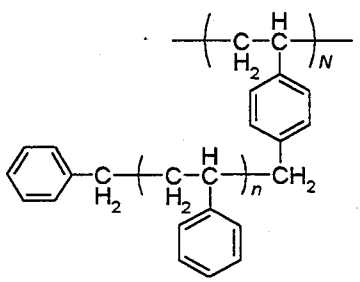

Figure I-2. Chemical structure of a polymacromonomer consisting only of polystyrene.

I. 2 Scope of This Work

We prepared two series of polymacromonomer samples consisting only of PS with n = 15 and 33 (designated throughout this thesis as F15 and F33, respectively). In parallel with the present work, Takeo[30] also synthesized F33 samples, and found from light scattering measurements on two samples with molecular weights of 2×10^5 and 3×10^5 that A_2 in cyclohexane vanishes around 34.5°C, the Θ temperature for linear PS in the same solvent. This was very encouraging in that the presence of the Θ condition should allow an unequivocal characterization of our polymacromonomers. Thus, our measurements began with determining the precise Θ temperatures for the two polymacromonomers in cyclohexane.

Chapter II following this introductory chapter describes experimental details, i.e., the synthesis and fractionation of the polymacromonomers, light scattering photometry, viscometry, and gel permeation chromatography. The light scattering and viscosity experiments in toluene were carried out at 15°C since the unperturbed dimensions and hence the chain stiffness of linear PS in this good solvent is known to agree essentially with those in cyclohexane at the Θ point.[7]

Chapters III and IV present light scattering results and their analyses. In the former, the Θ temperatures of our polymacromonomers in cyclohexane are determined from the temperature dependence of A_2, and the molecular weight dependence of $\langle S^2\rangle_z$ for each polymer is analyzed on the basis of the wormlike chain model to estimate the chain stiffness and the contour length

per main-chain residue. In the latter, $\langle S^2 \rangle_z$ data in cyclohexane at temperatures other than Θ and in toluene at 15°C are similarly analyzed, but excluded-volume effects are taken into consideration in the framework of the QTP theory.[2,4,5] The question is whether the chain stiffness changes when the solvent condition varies from the Θ state to toluene, a good solvent, i.e., when side chain – side chain or side chain – main chain repulsions are enhanced.

Chapter V is concerned with the viscosity behavior of the polymacromonomers in cyclohexane at the Θ point and in toluene. It is shown that the wormlike chain with or without excluded volume is capable of consistently explaining the $[\eta]$ and $\langle S^2 \rangle_z$ data for the polymers in both Θ and good solvents if the contribution of side chains near the main-chain ends to $[\eta]$ are taken into account.

Chapter VI summarizes main findings and conclusions from this work.

References

1. O. Kratky and G. Porod, *Rec. Trav. Chim.*, **68**, 1106 (1949).
2. H. Yamakawa, *Helical Wormlike Chains in Polymer Solutions*, Springer, Berlin, 1997.
3. T. Norisuye, *Prog. Polym. Sci.*, **18**, 543 (1993).
4. H. Yamakawa and W. H. Stockmayer, *J. Chem. Phys.*, **57**, 2843 (1972).
5. J. Shimada and H. Yamakawa, *J. Chem. Phys.*, **85**, 591 (1986).
6. H. Yamakawa, *Modern Theory of Polymer Solutions*, Harper & Row, New York, 1971.
7. F. Abe, Y. Einaga, T. Yoshizaki, and H. Yamakawa, *Macromolecules*, **26**, 1884 (1993).
8. F. Abe, Y. Einaga, and H. Yamakawa, *Macromolecules*, **26**, 1891 (1993).
9. K. Horita, F. Abe, Y. Einaga, and H. Yamakawa, *Macromolecules*, **26**, 5067 (1993).
10. F. Abe, K. Horita, Y. Einaga, and H. Yamakawa, *Macromolecules*, **27**, 725 (1994).
11. M. Kamijo, F. Abe, Y. Einaga, and H. Yamakawa, *Macromolecules*, **28**, 1095 (1995).
12. T. Norisuye, A. Tsuboi, and A. Teramoto, *Polym. J.*, **28**, 357 (1996).
13. J. F. Douglas, J. Roovers, and K. F. Freed, *Macromolecules*, **23**, 4168 (1990).
14. G. S. Grest, L. J. Fetters, J. S. Huang, and D. Richter, *Adv. Chem. Phys.*, **94**, 67 (1996).
15. B. H. Zimm and W. H. Stockmayer, *J. Chem. Phys.*, **17**, 1301 (1949).
16. B. H. Zimm and R. W. Kilb, *J. Chem. Phys.*, **37**, 19 (1959).
17. W. H. Stockmayer and M. Fixman, *Ann. N. Y. Acad. Sci.*, **57**, 334 (1953).
18. M. Okumoto, Y. Nakamura, T. Norisuye, and A. Teramoto, *Macromolecules*, **31**, 1615 (1998).
19. M. Okumoto, K. Terao, Y. Nakamura, T. Norisuye, and A. Teramoto, *Macromolecules*, **30**, 7493 (1997).
20. I. Noda, T. Horikawa, T. Kato, T. Fujimoto, and M. Nagasawa, *Macro-*

molecules, **3**, 795 (1970).

21. See, for example, Y. Nakamura, T. Norisuye, and A. Teramoto, *Macromolecules*, **24**, 4904 (1991).
22. E. F. Cassasa and G. C. Berry, *J. Polym. Sci.*, Part A-2, **4**, 881 (1966).
23. Y. Tsukahara, K. Mizuno, A. Segawa, and Y. Yamashita, *Macromolecules*, **22**, 1546 (1989).
24. Y. Tsukahara, K. Tsutsumi, Y. Yamashita, and S. Shimada, *Macromolecules*, **23**, 5201 (1990).
25. Y. Tsukahara, in *Macromolecular Design: Concept and Practice*, M. K. Mishra Ed., Polymer Frontiers International Inc., New York, 1994, pp. 161 – 227.
26. M. Wintermantel, M. Schmidt, Y. Tsukahara, K. Kajiwara, and S. Kohjiya, *Macromol. Rapid Commun.*, **15**, 279 (1994).
27. M. Wintermantel, M. Gerle, K. Fischer, M. Schmidt, I. Wataoka, H. Urakawa, K. Kajiwara, and Y. Tsukahara, *Macromolecules*, **29**, 978 (1996).
28. N. Nemoto, M. Nagai, A. Koike, and S. Okada, *Macromolecules*, **28**, 3854 (1995).
29. Y. Tsukahara, J. Inoue, Y. Ohta, S. Kohjiya, and Y. Okamoto, *Polym. J.*, **26**, 1013 (1994).
30. Y. Takeo, M. S. Thesis, Osaka University, 1997.

Chapter II Experimental

II. 1 Polymacromonomer Samples

II. 1. 1 Synthesis of Polystyrene Macromonomer

α-Benzyl-ω-vinylbenzyl (atactic) polystyrene, a macromonomer, was synthesized by living anionic polymerization of styrene at room temperature under Ar atmosphere with *n*-butyllithium (*n*-BuLi)/tetrametylethylenediamine (TMEDA)/toluene ligand complex as an initiator (Scheme II-1); the styrene concentration was about 15%. This complex had been prepared by mixing TMEDA with an *n*-BuLi/toluene solution at a molar concentration ratio [TMEDA] / [BuLi] of 1.3. The polymerization was terminated with a tetrahydrofuran solution of *p*-vinylbenzyl chloride (VBCl) at –78°C ([VBCl] / [BuLi] = 3.5) and the reaction mixture was stirred for 8 h at room temperature. The product (designated as MM15) was reprecipitated 5 times from acetone solutions into methanol to remove unreacted VBCl, and dried under vacuum at room temperature. Termination was also carried out with methanol to produce a precursor polystyrene (designated as P15) as shown in Scheme II-1. A similar macromonomer MM33 and its precursor polystyrene P33 were synthesized by Takeo.[1] These were also used for the present work.

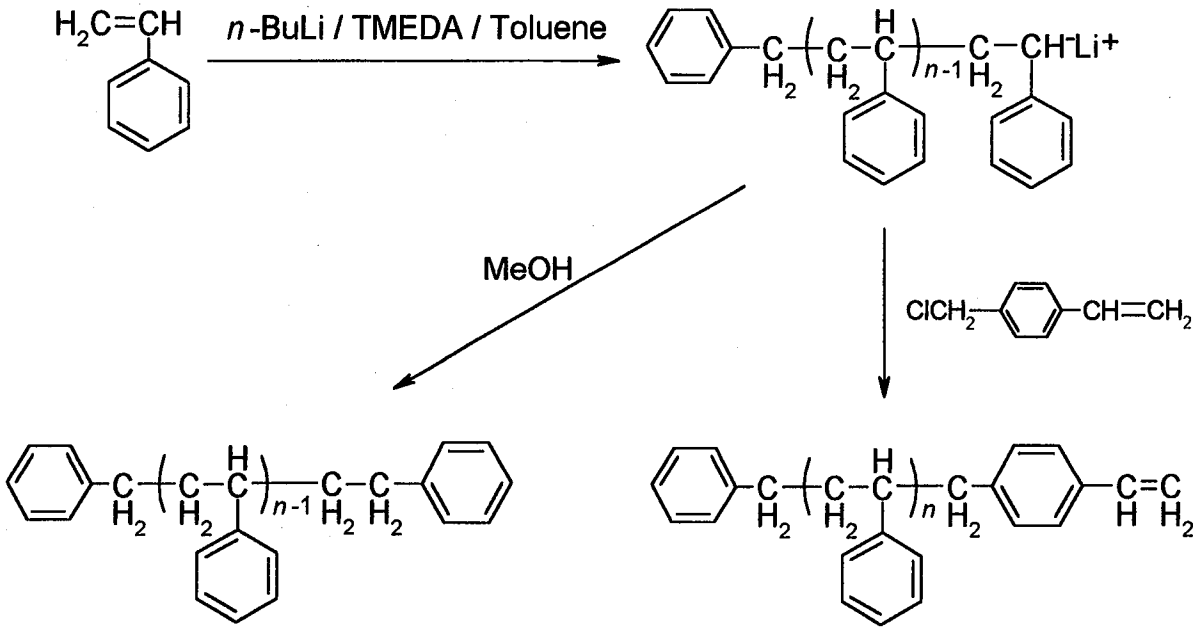

Scheme II-1.

II. 1. 2 Characterization of Precursors and Macromonomers

The weight-average molecular weights M_w of the precursors P15 and P33 were determined by light scattering in cyclohexane at 34.5°C, using vertically polarized incident light of 436-nm wavelength (see Section II. 4). The specific refractive index increments $\partial n/\partial c$ determined were 0.185 and 0.184 cm^3g^{-1} for P15 and P33, respectively (see Section II. 3 for the experimental procedure). Weight-average to number-average molecular weight ratios M_w/M_n (M_w and number-average molecular weights M_n, as well) for these polymers were estimated by a MALDI-TOF-mass spectrometer with a *trans*, *trans*-1,4-diphenyl-1,3-butadiene matrix containing silver ions in form of $AgCF_3COO$. The molecular weight data are summarized in Table II-1. It can be seen that the M_w values from light scattering and mass spectroscopy are in good agreement and that both P15 and P33 are narrow in molecular weight distribution.

Table II-1. Characterization of the Precursors (α-Benzyl-ω-hydrogen Polystyrenes)

	Light Scattering	MALDI-TOF		
Precursor	$M_w/10^3$	$M_w/10^3$	$M_n/10^3$	M_w/M_n
P15	1.53	1.59	1.46	1.09
P33	3.44	3.32	3.21	1.03

The molecular weights of the macromonomers MM15 and MM33 were evaluated from the light scattering M_w values for their precursors P15 and P33. They are presented in Table II-2.

^{1}H NMR spectra were taken on a JOEL JNM-LA-500 spectrometer for the macromonomer MM15 and the precursor P15 in $CDCl_3$ at 55°C to characterize the end group. The polymer concentration was adjusted to 10 wt%.

Figure II-1(a) shows the ^{1}H NMR spectrum for P15. It can be seen that there is no peak at 0.5 – 0.8 ppm corresponding to the methyl protons[2] of the initiator residue of *n*-BuLi. This implies that the benzyl group at the α-chain end was quantitatively introduced. The ^{1}H NMR spectrum of the macromonomer MM15 is shown in Figure II-1(b). The two peaks at 5.1 and 5.6 ppm correspond to the vinyl protons at the ω-end group. The end group functionality F of this macromonomer sample was estimated from their integrated intensities (the areas) to those for the phenyl proton peaks (6.3 – 7.3

Table II-2. Characterization of the Macromonomers (α-Benzyl-ω-vinyl-benzyl Polystyrenes)

Macromonomer	Molecular weight / 10^3 [a]	F [b]
MM15	1.65	0.75
MM33	3.56	0.73 [c]

[a] Calculated from M_w of the precursor

[b] ω-End group functionality

[c] Ref. 1

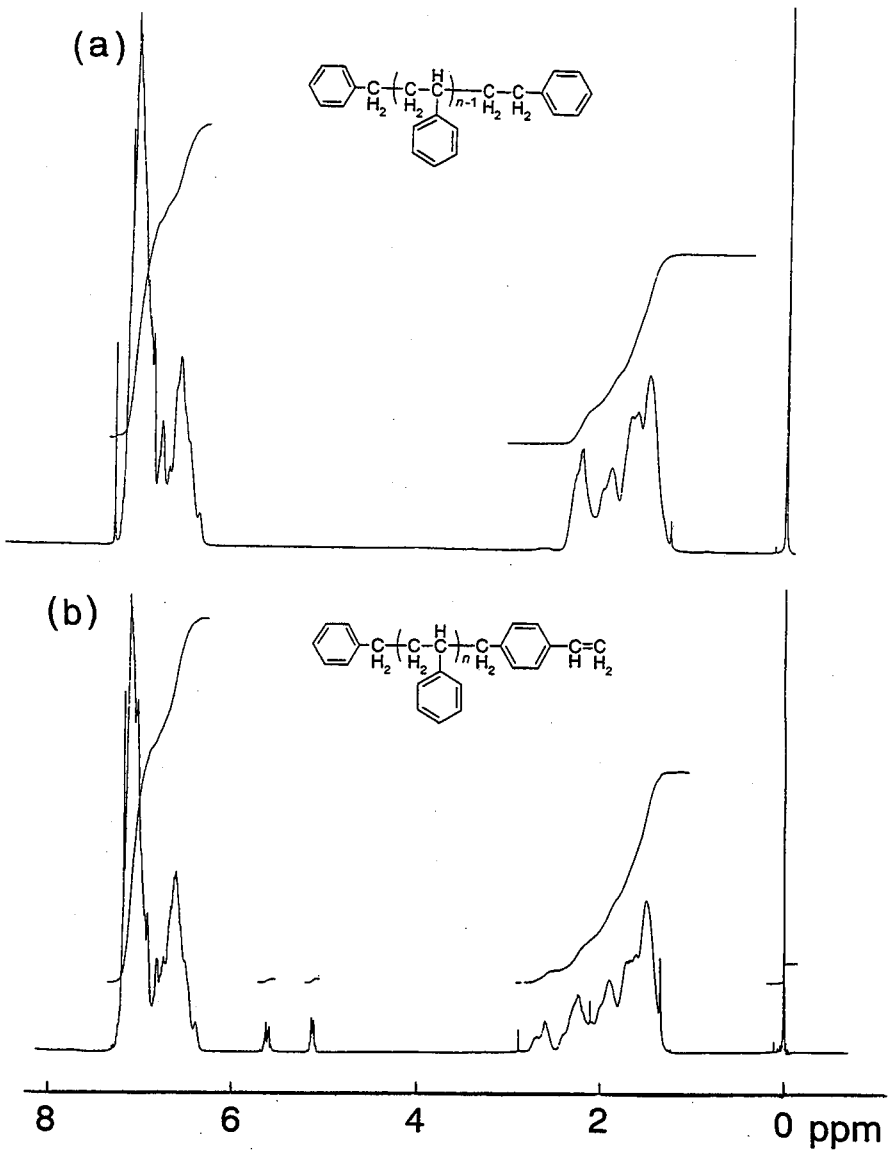

Figure II-1. ^{1}H NMR spectra of (a) α-benzyl-ω-hydrogen polystyrene (P15) and (b) α-benzyl-ω-vinylbenzyl polystyrene macromonomer (MM15).

ppm) with the aid of the molecular weight of MM15. The resulting F value is presented in the third column of Table II-2, along with Takeo's result for MM33.

II. 1. 3 Polymerization of the Macromonomers and Fractionation

Samples of F15

The macromonomer MM15 was polymerized in benzene at different temperatures T of 45 – 60°C under N_2 atmosphere for about 50 – 100 h with azobis(isobutyronitrile) as an initiator. The details of polymerization conditions and the results are summarized in Table II-3, along with the molecular weights M_{peak} determined from the peak times of GPC curves using the calibration curve for the polymacromonomer F15 (see Section II. 5).

Anionic polymerization was also carried out under Ar atmosphere with *n*-BuLi/TMEDA/toluene complex as an initiator to prepare five low molecular weight samples. The results are presented in Table II-4.

Figure II-2 shows typical GPC curves for (a) the macromonomer MM15, (b) the product from anionic polymerization (run No. 3 in Table II-4), and (c) the product from radical polymerization (run No. 6 in Table II-3). The left peaks in (b) and (c) correspond to the polymacromonomers, while the right peaks correspond to the unreacted macromonomer. The molecular weight of the anionic-polymerization product is seen to be much lower than that of the radical-polymerization product (see also Tables II-3 and II-4).

Table II-3. Radical Polymerizations of the Polystyrene Macromonomers

Run	Monomer	[M] [a] mol l^{-1}	[I] [b] mol l^{-1}	Temp. °C	Time h	Conversion %	M_{peak} [c] 10^5
1	MM15	0.43	0.085	60	48	65	3.7
2	MM15	0.38	0.080	60	72	70	4.2
3	MM15	0.38	0.070	60	50	65	3.8
4	MM15	0.43	0.017	60	48	70	5.1
5	MM15	0.42	0.017	60	48	60	6.3
6	MM15	0.43	0.009	60	48	70	5.0
7	MM15	0.43	0.009	60	50	65	5.5
8	MM15	0.43	0.017	45	96	70	10
9	MM15	0.43	0.009	45	72	50	13
10	MM15	0.43	0.005	40	110	50	20
11	MM15	0.43	0.004	40	100	45	21
12	MM15	0.43	0.009	35	96	13	18
13	MM33	0.18	0.004	40	110	45	30

[a] Macromonomer concentration

[b] Initiator concentration

[c] Determined from the peak time of the GPC curve

Table II-4. Anionic Polymerizations of the Polystyrene Macromonomers

Run	Monomer	[M] [a]	[I] [b]	Time	Conversion	M_{peak} [c]
		mol l^{-1}	mmol l^{-1}	h	%	10^4
1	MM15	0.12	0.100	24	64	0.51
2	MM15	0.12	0.062	24	73	1.1
3	MM15	0.12	0.028	6	49	2.6
4	MM15	0.12	0.021	24	56	4.7
5	MM15	0.24	0.034	24	71	6.1
6	MM33	0.11	0.060	24	70	5.4
7	MM33	0.11	0.040	40	37	13

[a] Macromonomer concentration

[b] Initiator concentration

[c] Determined from the peak time of the GPC curve

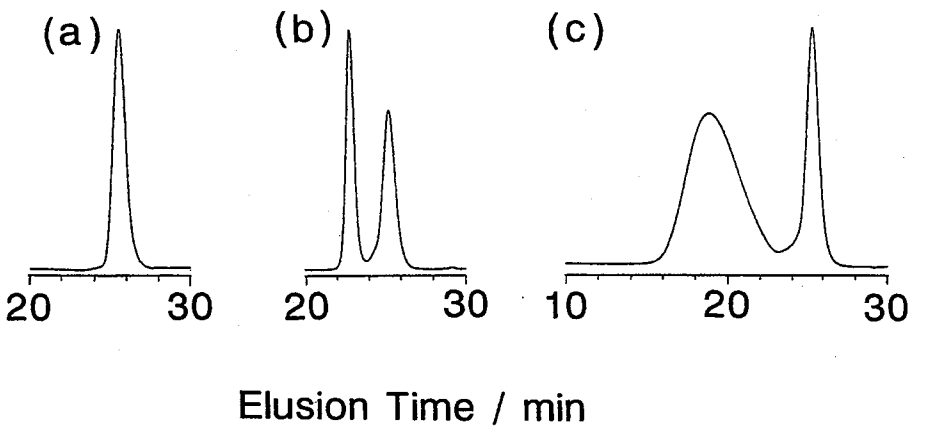

Figure II-2. GPC curves for (a) the macromonomer MM15, (b) a living anionic polymerization product, and (c) a radical polymerization product.

After unreacted macromonomers had been removed by fractional solution, the radical-polymerization products were divided each into a number of parts by repeated fractional precipitation with toluene as the solvent and methanol as the precipitant, or with cyclohexane at successively varying temperatures; when cooled below 32°C, cyclohexane solutions separated into two phases, and the phase separation was effective for fractionation of high molecular weight samples. From the fractions obtained, 10 middle ones designated below as F15-1, F15-2, ..., F15-10 were chosen for the present study.

The anionic-polymerization products were also fractionated by repeated fractional solution with toluene as the solvent and methanol as the precipitant, and appropriate middle fractions designated as F15-11, F15-12, F15-13, F15-14, and F15-15 were added to the above-mentioned 10 samples.

Samples of F33

Radical polymerization of the macromonomer MM33 was carried out under the conditions given in Table II-3. Probably because of the low polymerization temperature 40°C, it yielded a very high M_{peak} of 3×10^6, which is indeed more than 5 times as large as those reached by Takeo.[1] Our product was purified and extensively fractionated by the procedures employed for F15 samples, and from the fractions thus obtained, 9 middle ones designated as F33-1, F33-2, ..., F33-8, and F33-10 were chosen for the present study. Three samples, SS33-224, SS33-84, SS33-54, polymerized and fractionated by Takeo[1] were also used in this work under the names of F33-9, F33-11, and F33-12, respectively.

Two samples designated F33-13 and F33-14 were added to them. They were prepared by living anionic polymerization, followed by repeated fractional solution, in the manner described above for low molecular weight samples of F15. The polymerization conditions are given in Table II-4.

II. 2 Preparation of Solutions

Two solvents, cyclohexane and toluene, used in light scattering and viscometry were refluxed over sodium for about 5 h and then fractionally distilled. Polymacromonomer samples dried in vacuum were mixed with either solvent under stirring for 1 – 4 days at 40 – 50°C (for cyclohexane solutions) or at room temperature (for toluene solutions).

The polymer mass concentration c in units of g/cm^{-3} was calculated from

the gravimetrically determined polymer weight fraction w with the solution density ρ. Densities of cyclohexane solutions of the polymacromonomers F15 and F33 at 25, 35, and 45°C and those of toluene solutions at 15°C were determined for samples F15-10, F15-13, F15-15, and F33-13 using a Lipkin-Davison type pycnometer with 7 cm^3 capacity. Figure II-3 shows that the ρ

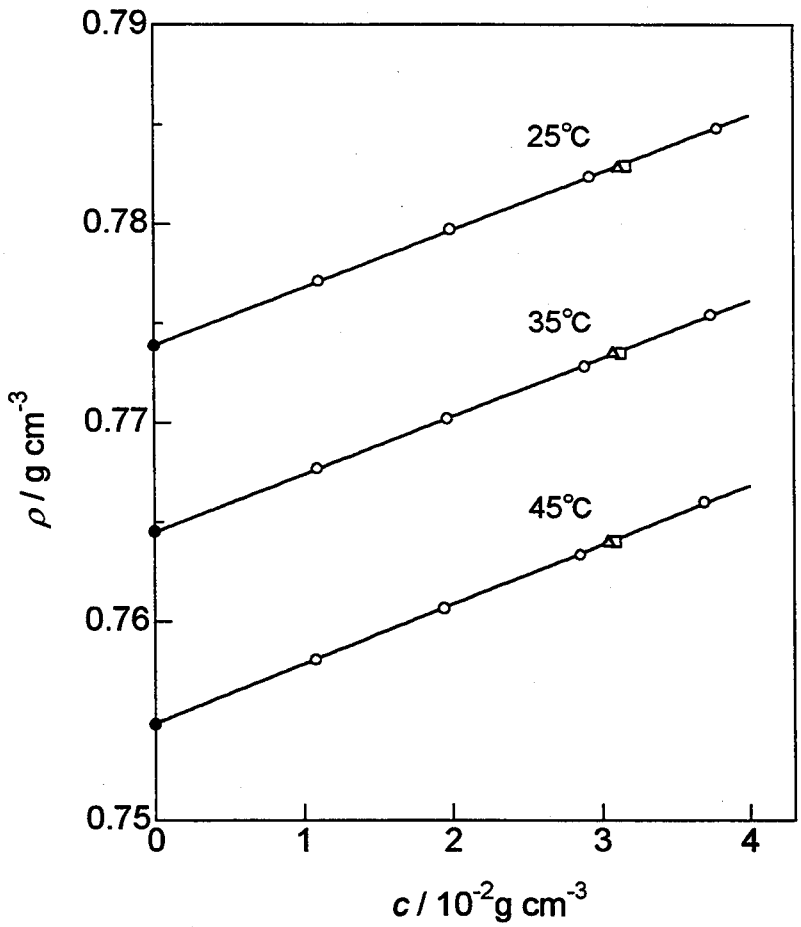

Figure II-3. Concentration dependence of solution density ρ for the polymacromonomer F15 in cyclohexane at the indicated temperatures: (□), F15-10; (○), F15-13; (△), F15-15; (●), pure cyclohexane.

vs. c plots for the polymacromonomer F15 in cyclohexane at the three temperatures are linear throughout the concentration range studied, giving

$$\rho = \rho_0 + (\partial\rho/\partial c)c \qquad \text{(II-1)}$$

where ρ_0 denotes the solvent density and the density increment $\partial\rho/\partial c$ refers to infinite dilution. The values of ρ_0, $d\rho_0/dT$, $\partial\rho/\partial c$, and $d(\partial\rho/\partial c)/dT$ are summarized in Table II-5.

Table II-5. Densities of Solutions of the Polymacromonomers F15 and F33

			ρ_0	$d\rho_0/dT$		$d(\partial\rho/\partial c)/dT$
Polymer	Solvent	T/°C	g cm^{-3}	10^{-4}g cm^{-3}K^{-1}	$\partial\rho/\partial c$	10^{-4}K^{-1}
F15	CH [a]	35	0.7645	− 9.5	0.291	5
F15	Tol [b]	15	0.8716	—	0.208	—
F33	CH	35	0.7645	− 9.5	0.287	4
F33	Tol	15	0.8716	—	0.210	—

[a] Cyclohexane

[b] Toluene

II. 3 Specific Refractive Index Increment

Excess refractive indices Δn for the polymacromonomers F15 and F33 in cyclohexane at 25, 30, 35, and 40°C and in toluene at 15°C were measured for samples F15-5, F15-10, F15-13, and F33-13 using a modified Schulz-Cantow

type differential refractometer. The c dependence of Δn for the polymacromonomer F15 in toluene is illustrated in Figure II-4, and the results for $\partial n/\partial c$ are summarized in Table II-6.

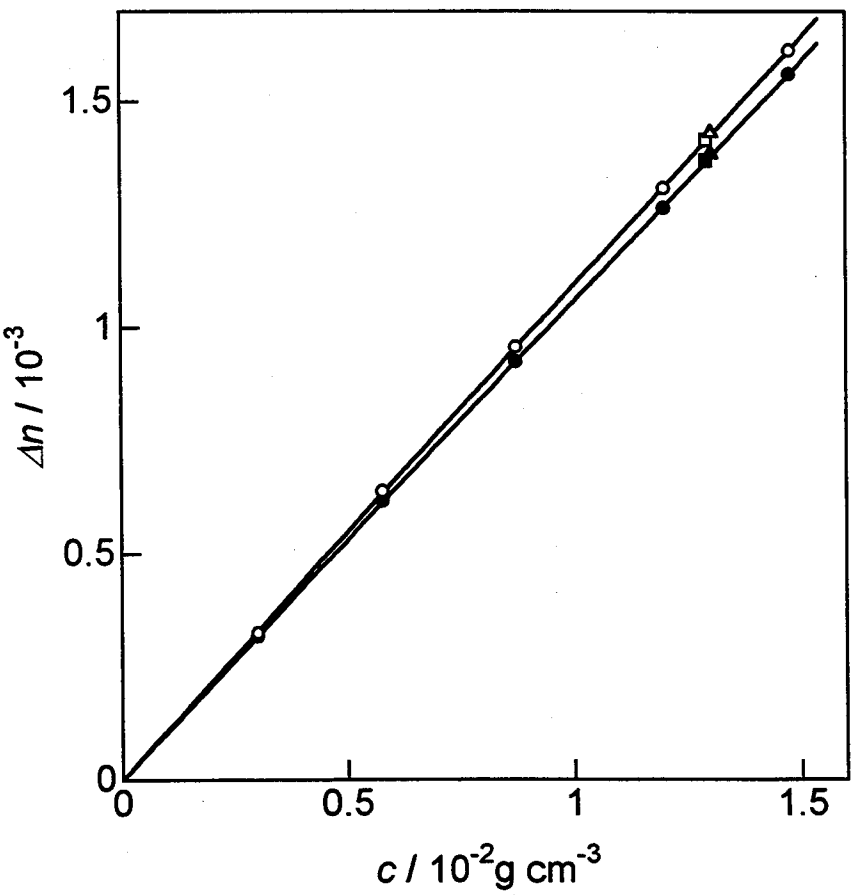

Figure II-4. Concentration dependence of excess refractive index Δn for the polymacromonomer F15 in toluene at 15°C: (○,●), F15-13; (△,▲), F15-5; (□,■), F15-10. The filled and unfilled symbols refer to the wavelengths of 546 and 436 nm, respectively.

Table II-6. Specific Refractive Index Increments for Solutions of the Polymacromonomers F15 and F33

			$(\partial n/\partial c)$ / cm^3g^{-1}		$d(\partial n/\partial c)/dT$ [c]
Polymer	Solvent	T/°C	436 nm	546 nm	10^{-4} $cm^3g^{-1}K^{-1}$
F15	CH [a]	34.5	0.184	0.171	3.6
F15	Tol [b]	15	0.110	0.106	—
F33	CH	34.5	0.182	0.170	4.0
F33	Tol	15	0.109	0.105	—

[a] Cyclohexane

[b] Toluene

[c] For both 436 and 546 nm

II. 4 Light Scattering Photometry

II. 4. 1 Measurement

Scattering intensities $I_{\theta,Uv}$ were measured for all polymacromonomer samples in toluene at 15°C and fifteen samples (F15-1, F15-2, ..., F15-6, F15-8, F15-12, F33-1, F33-2, F33-3, F33-4, F33-6, F33-7, and F33-9) in cyclohexane at different temperatures on a Fica-50 light scattering photometer in an angular range from 15 to 150°, using vertically polarized incident light of 436 and 546-nm wavelengths. Here, $I_{\theta,Uv}$ denotes the scattering intensity measured at scattering angle θ with a vertically oriented polarizer and no analyzer.

The reduced scattering intensity $R_{\theta,Uv}$ was calculated from the excess

scattering intensity $\Delta I_{\theta,Uv}$ using

$$R_{\theta,Uv} = \Phi \Delta I_{\theta,Uv} n_0^2 \sin\theta \qquad \text{(II-2)}$$

Here, Φ is the instrument constant and n_0 is the refractive index of the solvent. The former was determined from the measured intensity $I_{b,Uv}$ for benzene at 25°C and $\theta = 90°$ by use of the equation

$$\Phi = \frac{2R_{b,Uu}}{I_{b,Uv} n_b^2 (1+\rho_u)} \qquad \text{(II-3)}$$

with $R_{b,Uu}$ (the Rayleigh ratio of the liquid for unpolarized light) taken as[3] 46.5×10^{-6} cm^{-1} for 436 nm and 16.1×10^{-6} cm^{-1} for 546 nm (n_b denotes the refractive index of benzene). The depolarization ratio ρ_u of this liquid for unpolarized incident light was determined to be 0.41 and 0.40 for 436 and 546 nm, respectively, by the method of Rubingh and Yu.[4]

The optical anisotropy of our polymacromonomers was investigated for samples F15-4, F15-8, F15-12, F33-4, and F33-7 in cyclohexane at different temperatures and for samples F15-10, F15-15, F33-8, and F33-14 in toluene at 15°C. When the light scattering envelopes observed with the analyzer set in the vertical direction and without analyzer were compared, no difference was detected for any of these samples. Furthermore, the scattered intensity of the lowest molecular weight sample F15-15 in toluene measured with the analyzer set in the horizontal direction was not more than 0.4% of the intensity

measured with no analyzer, at every angle studied. From these results the optical anisotropy of the polymacromonomers was concluded to be negligible in the range of molecular weight studied, and no anisotropy correction was applied to any of light scattering data obtained in this work.

Polymer solutions and the solvents (cyclohexane and toluene) were made optically clean by centrifugation at about 3×10^4 gravities for 1.5 h. Each of them was transferred directly into the light scattering cell with a carefully cleaned pipet. The cell and the pipet had been rinsed with refluxing acetone vapor for about 6 h.

II. 4. 2 Data Analysis

According to the theory of light scattering from dilute solutions of an optically isotropic polymer, $R_\theta (\equiv R_{\theta,\mathrm{Uv}})$ is expressed by[5]

$$\frac{Kc}{R_\theta} = \frac{1}{M_\mathrm{w} P(\theta)} + 2A_2 Q(\theta) c + O\left(c^2\right) \qquad \text{(II-4)}$$

where $P(\theta)$ is the particle scattering function, $Q(\theta)$ is the factor related to intermolecular interference of scattered light, A_2 is the second virial coefficient, and K is the optical constant defined by

$$K = \frac{4\pi^2 n^2}{N_A \lambda_0^4}\left(\frac{\partial n}{\partial c}\right)^2 \qquad \text{(II-5)}$$

wherein n is the refractive index of the polymer solution, N_A is the Avogadro constant, and λ_0 is the wavelength of incident light in vacuum. At infinite dilution, eq II-4 can be rewritten as[6]

$$\left(\frac{Kc}{R_\theta}\right)_{c=0}^{1/2} = \left(\frac{1}{M_w P(\theta)}\right)^{1/2} = \frac{1}{M_w^{1/2}}\left[1 + \frac{1}{6}\left(\frac{4\pi n_0}{\lambda_0}\right)^2 <S^2>_z \sin^2\frac{\theta}{2} + O\left(\sin^4\frac{\theta}{2}\right)\right] \qquad \text{(II-6)}$$

Here, $<S^2>_z$ is the z-average mean-square radius of gyration of the polymer. In the limit of $\theta = 0$, eq II-4 is reduced to[5,6]

$$\frac{Kc}{R_0} = \frac{1}{M_w} + 2A_2 c + O(c^2) \qquad \text{(II-7)}$$

or

$$\left(\frac{Kc}{R_0}\right)^{1/2} = \frac{1}{M_w^{1/2}}\left[1 + A_2 M_w c + O(c^2)\right] \qquad \text{(II-8)}$$

where R_0 is the scattering intensity at $\theta = 0$.

On the basis of the above equations, the scattering intensity data obtained were analyzed by use of the square-root plots of $(Kc/R_\theta)^{1/2}$ vs. c and

$(Kc/R_\theta)^{1/2}$ vs. $\sin^2(\theta/2)$, but for the concentration dependence of intensity for cyclohexane solutions, the linear plot of Kc/R_θ vs. c was used. The values of A_2 for these solutions were determined from the data at 546 nm, since, as remarked elsewhere,[7] the attenuation of light by scattering, absorption, and multiple scattering were not always negligible at 436 nm, giving rise to small errors (less than 10^{-5} mol cm^3g^{-2}) in A_2 near the Θ point.

II. 5 Viscometry

Viscosity measurements in cyclohexane at 34.5°C and in toluene at 15°C were made using a four-bulb low-shear capillary viscometer of the Ubbelohde type for samples F15-1, F15-2, F33-1, and F33-2 in toluene and conventional capillary viscometers for the rest; shear-rate effects on intrinsic viscosity $[\eta]$ were small (less than 1%) when the $[\eta]$ values for the four samples from the two types of viscometer were compared. Samples F33-1 and F33-2 in cyclohexane were not studied because they did not completely dissolve in the solvent at c (higher than 4×10^{-3} g cm^{-3}) desirable for our viscometry. We note that the lowest c required was 20 times higher than the highest c studied by light scattering since $[\eta]$ in cyclohexane at 34.5°C is quite small even for high M_w (see Chapter V).

In all measurements, the flow time was determined to a precision of 0.1 s with the difference between the solvent and solution flow times kept lager than 15 s. The relative viscosity was evaluated by taking account of the difference between the solution and solvent densities. The Huggins plot,[8]

the Fuoss-Mead plot,[9] and the Billmeyer plot[10] were combined to determine $[\eta]$ and the Huggins constant k'.

II. 6 Gel Permeation Chromatography

Polymacromonomer samples were analyzed by gel permeation chromatography (GPC) using an analytical gel permeation chromatograph TOSOH HLC8020 equipped with a UV detector operating at 254 nm under the following conditions: three TOSOH columns, TSK G6000HxL, TSK G5000HxL, and TSK G4000HxL, connected in series, chloroform at 40°C as the eluent, and a flow rate of 1 cm^3/min.

Figure II-5 shows the GPC calibration curves for the polymacromonomers F15 and F33, where the values of M_w were determined by light scattering (see Chapter IV). The polydispersity index M_w/M_n evaluated from the GPC curve for each fractionated sample is summarized in Table II-7; for fractions F15-1, F15-14, F15-15, F33-1, F33-12, F33-13, and F33-14, the evaluation was impossible because the calibration curves did not completely cover the GPC curves. It can be seen from the table that all the fractions examined by GPC are narrow in molecular weight distribution. Though not shown here, their z-average to weight-average molecular weight ratios were essentially the same as the M_w/M_n values.

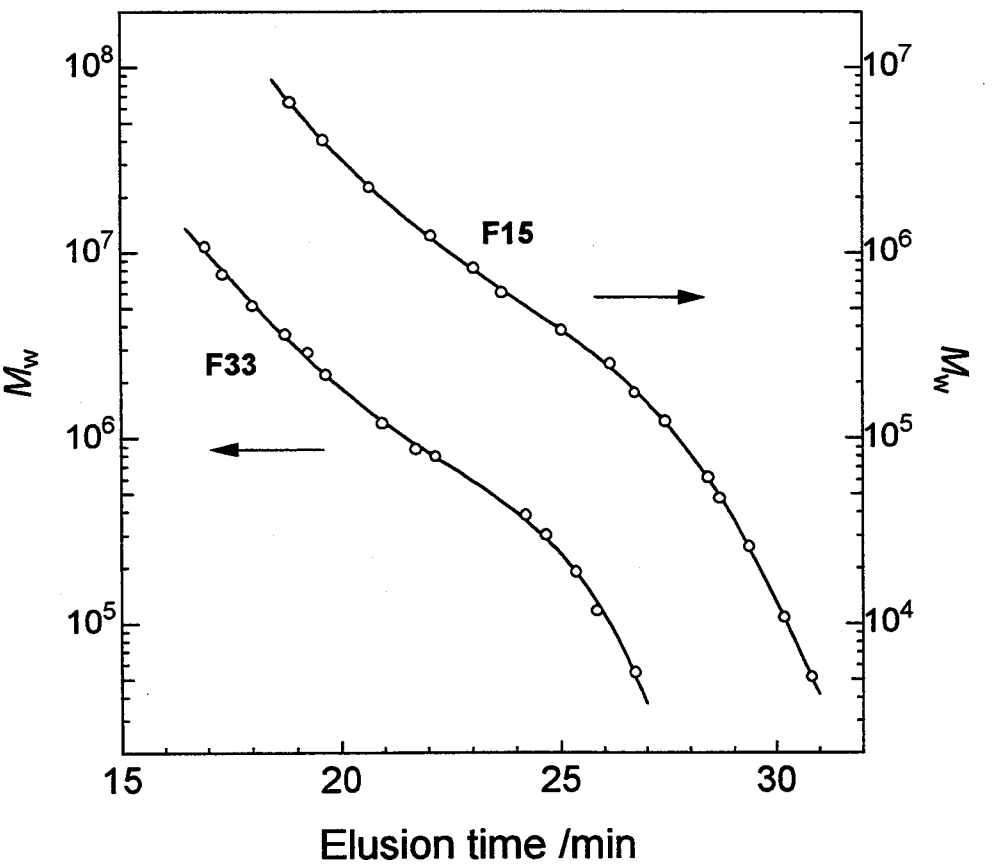

Figure II-5. GPC calibration curves for the polymacromonomers F15 and F33. Eluent, chloroform at 40°C.

Table II-7. Results from GPC Measurements

Sample	M_w/M_n	Sample	M_w/M_n
F15-2	1.08	F33-2	1.10
F15-3	1.07	F33-3	1.08
F15-4	1.06	F33-4	1.06
F15-5	1.05	F33-5	1.06
F15-6	1.06	F33-6	1.06
F15-7	1.08	F33-7	1.04
F15-8	1.09	F33-8	1.10
F15-9	1.10	F33-9	1.05
F15-10	1.10	F33-10	1.12
F15-11	1.08	F33-11	1.19
F15-12	1.09		
F15-13	1.09		

References

1. Y. Takeo, M. S. Thesis, Osaka University, 1997.
2. Y. Tsukahara, J. Inoue, Y. Ohta, S. Kohjiya, and Y. Okamoto, *Polym. J.*, **26**, 1013 (1994).
3. Gj. Deželić and J. Vavra, *Croat. Chem. Acta*, **38**, 35 (1966).
4. D. N. Rubingh and H. Yu, *Macromolecules*, **9**, 681 (1976).
5. B. H. Zimm, *J. Chem. Phys.*, **16**, 1093 (1948).
6. G. C. Berry, *J. Chem. Phys.*, **44**, 4550 (1966).
7. M. Okumoto, K. Terao, Y. Nakamura, T. Norisuye, and A. Teramoto, *Macromolecules*, **30**, 7493 (1997).
8. M. L. Huggins, *J. Am. Chem. Soc.*, **64**, 2716 (1942).
9. D. F. Mead and R. M. Fuoss, *J. Am. Chem. Soc.*, **64**, 277 (1942).
10. F. W. Billmeyer Jr., *J. Polym. Sci.*, **4**, 83 (1949).

Chapter III Light Scattering Characterization in Cyclohexane at the Θ Point

III. 1 Introduction

This chapter is concerned with light scattering characterization of two polymacromonomers (F15 and F33) consisting of polystyrene (PS) in cyclohexane at the Θ point. The primary purpose is to examine the effect of side chain length on main chain stiffness, i.e., how stiff these polymers in the Θ state are in comparison with linear PS. This is a first step toward understanding the effects of molecular architecture and intramolecular interactions on chain stiffness. We first determine the Θ temperatures for the respective polymacromonomers from the temperature dependence of second virial coefficient A_2 in cyclohexane and then analyze the z-average mean-square radii of gyration $\langle S^2 \rangle_z$ in cyclohexane obtained as functions of weight-average molecular weight M_w at each Θ temperature, on the basis of the Kratky-Porod wormlike chain.[1]

III. 2 Results

III. 2. 1 Second Virial Coefficient and Θ Temperature

Polymacromonomer F15

Figure III-1 illustrates plots of $(Kc/R_\theta)^{1/2}$ vs. $\sin^2(\theta/2)$ at fixed polymer

mass concentrations c for sample F15-4 in cyclohexane at 34.5°C. Here, K is the optical constant and R_θ the reduced scattering intensity at scattering angle θ. The zero-angle values of Kc/R_θ, i.e., Kc/R_0, obtained at this and other temperatures T are plotted against c in Figure III-2. The straight lines fitting the plotted points at the respective T converge to a common intercept, yielding an identical M_W within experimental error. The slope and hence A_2 change from negative to positive with increasing T. This can be seen more clearly in Figure III-3, in which the A_2 data for the sample are plotted against T, along with those for samples F15-8 and F15-12. The virial coefficients for the three samples vanish around 34.5°C, the Θ temperature for linear PS in

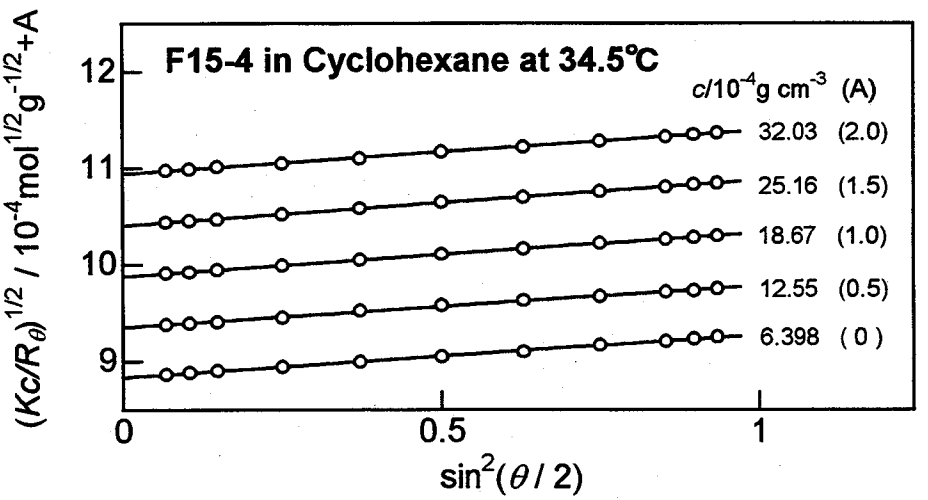

Figure III-1. Plots of $(Kc/R_\theta)^{1/2}$ vs. $\sin^2(\theta/2)$ at indicated c for polymacromonomer sample F15-4 in cyclohexane at 34.5°C. Wavelength, 546 nm. For clarity, the ordinate values at each c are shifted by A.

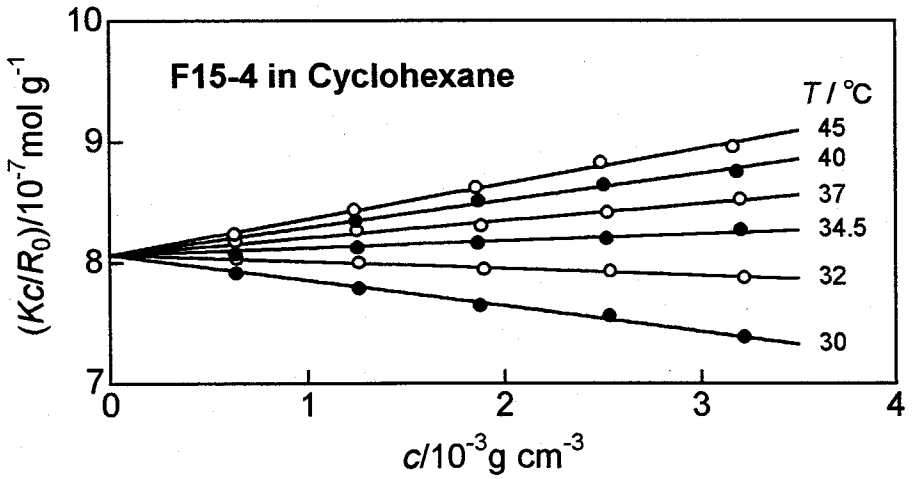

Figure III-2. Concentration dependence of Kc/R_0 for polymacromonomer sample F15-4 in cyclohexane at indicated temperatures. Wavelength, 546 nm.

cyclohexane.[2] Thus, we find that the polymacromonomer F15 in cyclohexane has a Θ point at essentially the same temperature as that for the linear chain. With regard to the precision of the Θ temperature for the present system, the following remark may be pertinent.

As can be seen in Figure III-3 or from Table III-1 in which the numerical data are summarized, the T-dependence of A_2 is very weak (compared to that for linear PS[2]). In particular, A_2 for sample F15-4 stays less than 10^{-5} mol g^{-2} cm^3 over a range of T from 32 to 37°C. Such a T range extended more for a higher M_w (not shown here). In view of the T-insensitive behavior of A_2, it is probably safe to allow of an uncertainty of about ±1°C for the Θ point (34.5°C) of the polymacromonomer F15 + cyclohexane system.

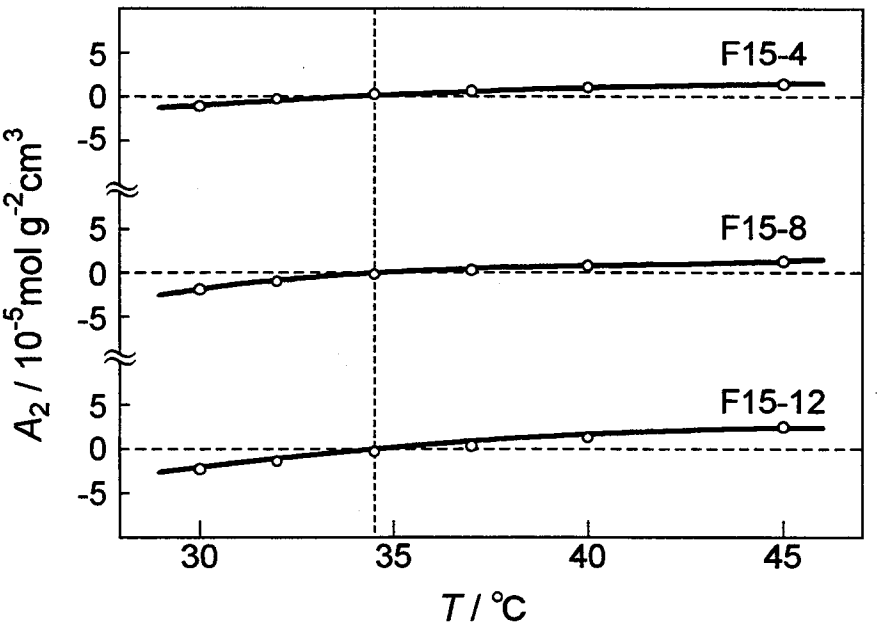

Figure III-3. Temperature dependence of A_2 for polymacromonomer samples F15-4, F15-8, and F15-12 in cyclohexane. The vertical dashed line indicates 34.5°C (the Θ temperature).

Table III-1. Values of A_2 for Polymacromonomer F15 Samples in Cyclohexane at Different Temperatures

		A_2 /10^{-5}mol $g^{-2}cm^3$					
Sample	$M_w/10^4$	30°C	32°C	34.5°C	37°C	40°C	45°C
F15-4	124	-1.1	-0.3	0.2	0.6	1.0	1.3
F15-8	25.4	-1.9	-1.0	-0.2	0.3	0.8	1.3
F15-12	4.70	-2.3	-1.4	-0.3	0.3	1.3	2.5

Polymacromonomer F33

As mentioned in Chapter I, Takeo[3] found for two samples of the polymacromonomer F33 with M_w = 1.9×10^5 and 3.0×10^5 that A_2 in cyclohexane vanishes around 34.5°C. Since these molecular weights are relatively low and too close to each other, we determined the temperature dependence of A_2 for a much higher molecular weight sample (F33-6) with $M_w = 2.2\times10^6$ in cyclohexane to confirm Takeo's finding. Our and his A_2 data are presented in Table III-2 and illustrated in Figure III-4. We see that the polymacromonomer F33 in cyclohexane attains the Θ condition at 34.5°C, as is the case with the polymacromonomer F15 and linear PS.[2] This strongly suggests that for polymacromonomers of the kind shown in Figure I-2, the Θ temperature is essentially independent of side chain length, at least, for n (degree of polymerization of each side chain) $\lesssim$ 33.

Interestingly, however, the T-dependence of A_2 in Figure III-4 is much

Table III-2. Values of A_2 for Polymacromonomer F33 Samples in Cyclohexane at Different Temperatures

		A_2 /10^{-5}mol g^{-2}cm^3						
Sample	$M_w/10^4$	25°C	30°C	32°C	34.5°C	37°C	40°C	45°C
F33-6	218		-0.3	-0.1	0.2	0.4	0.6	1.0
F33-11	30.0[a]	-2.0[a]	-0.8[a]	—	0[a]	—	1.6[a]	—
F33-12	18.9[a]	-1.8[a]	-0.5[a]	—	0[a]	—	1.5[a]	—

[a] Ref. 3

weaker than that for linear PS[2] and slightly weaker than that for the F15 polymer, so that an effect of side chain length appears in the magnitude of (dA_2/dT) at the Θ point. We note that because of the T-insensitive behavior of A_2, the Θ temperature of 34.5°C for the polymacromonomer F33 + cyclohexane system is accurate to about ±2°C.

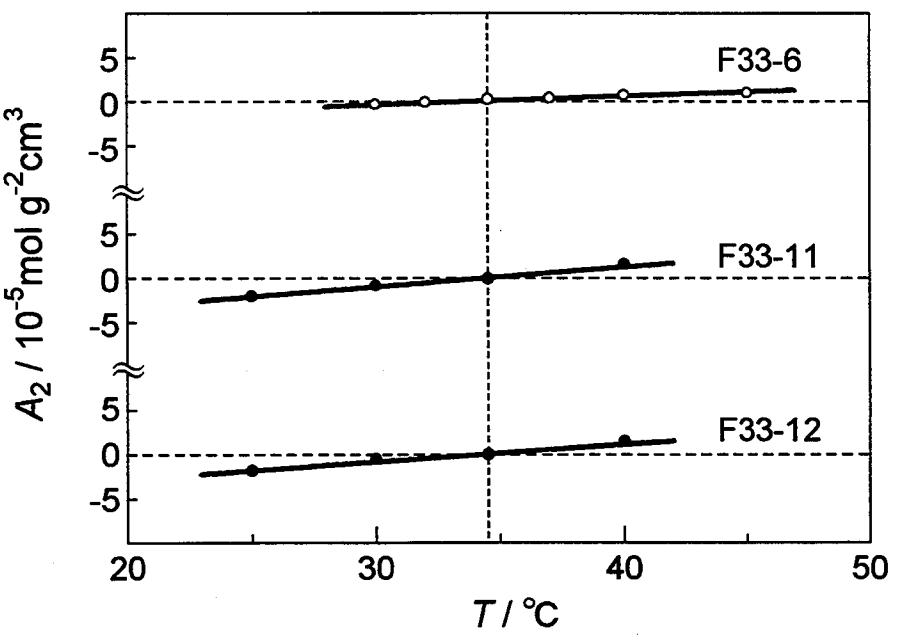

Figure III-4. Temperature dependence of A_2 for polymacromonomer samples F33-6 (○, this work), F33-11, and F33-12 (●, Takeo[3]) in cyclohexane. The vertical dashed line indicates 34.5°C (the Θ temperature).

III. 2. 2 Radius of Gyration at the Θ Temperature

Figures III-5 and III-6 show the angular dependence of $P(\theta)^{-1/2}$, i.e., $(M_w Kc/R_\theta)^{1/2}$ at infinite dilution, for samples of F15 and F33, respectively, in cyclohexane at 34.5°C. The values of $\langle S^2 \rangle_z$ evaluated from the initial slopes (the dashed lines) are summarized in Tables III-3 and III-4.

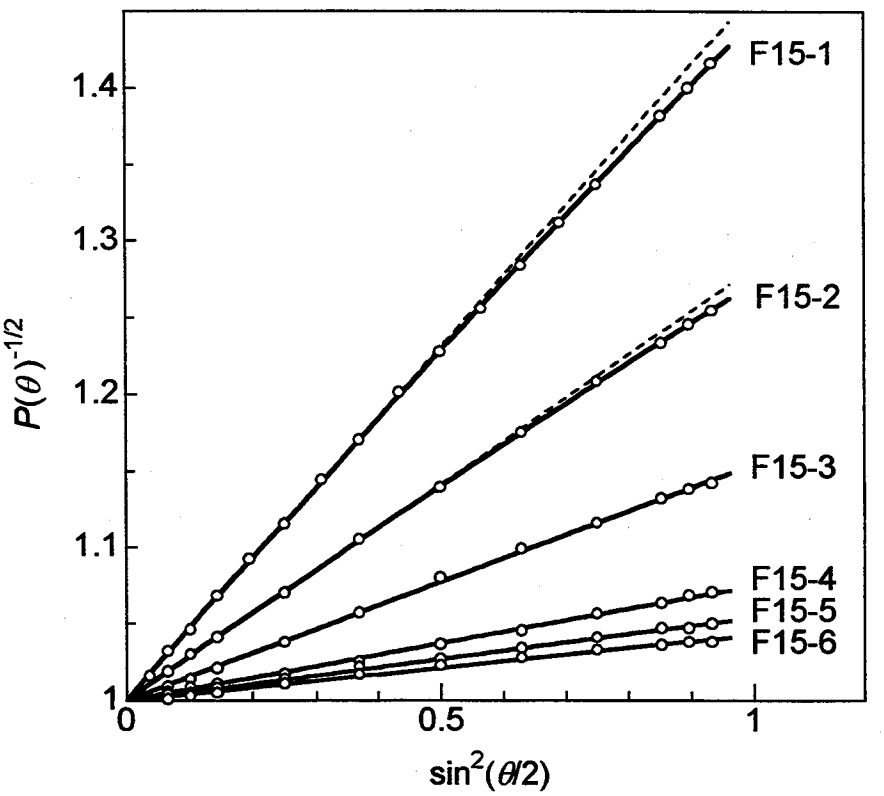

Figure III-5. Angular dependence of $P(\theta)^{-1/2}$ for indicated polymacromonomer F15 samples in cyclohexane at 34.5°C. Dashed lines, initial slopes; wavelength of incident light, 436 nm.

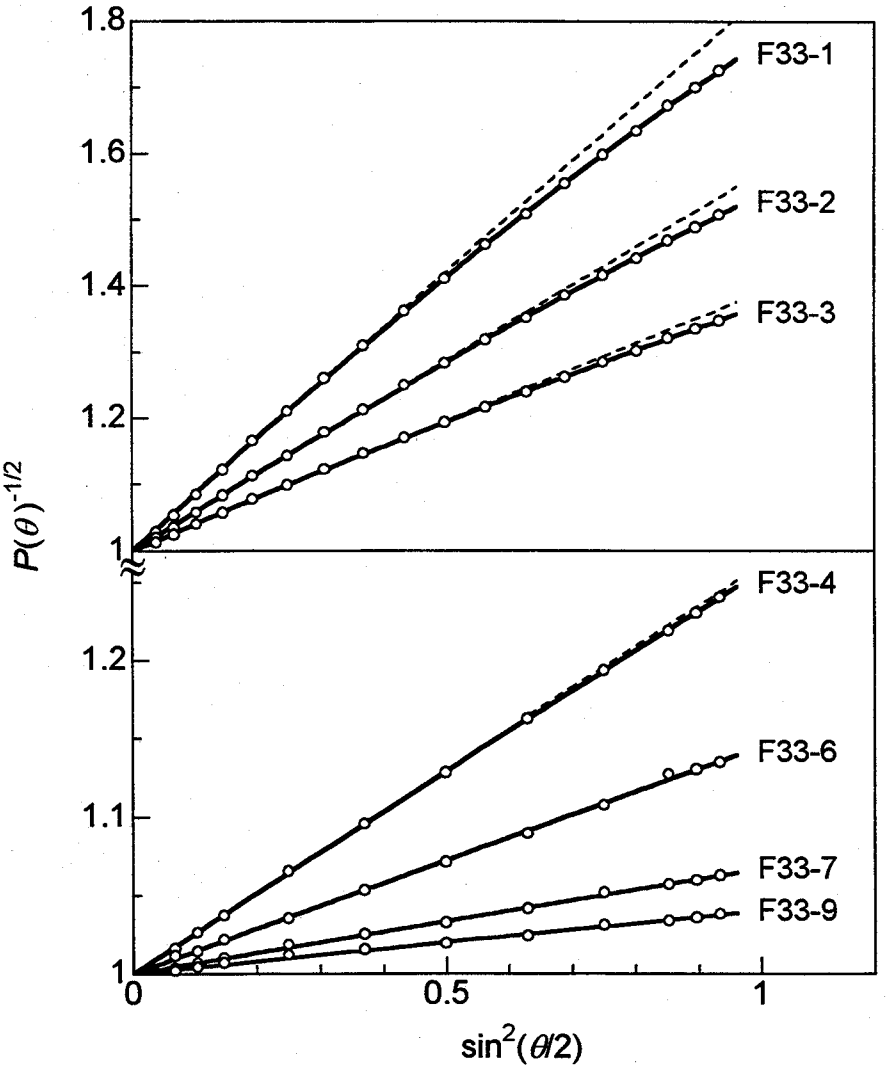

Figure III-6. Angular dependence of $P(\theta)^{-1/2}$ for indicated polymacromonomer F33 samples in cyclohexane at 34.5°C. Dashed lines, initial slopes; wavelength of incident light, 436 nm.

Table III-3. Values of $\langle S^2 \rangle_z$ for Polymacromonomer F15 Samples in Cyclohexane at 34.5°C

Sample	$M_w / 10^5$	$\langle S^2 \rangle_z / 10^2$ nm^2
F15-1	66.1	16.0
F15-2	39.8	9.80
F15-3	22.1	5.43
F15-4	12.4	2.86
F15-5	8.41	1.90
F15-6	6.29	1.39

Table III-4. Values of $\langle S^2 \rangle_z$ for Polymacromonomer F33 Samples in Cyclohexane at 34.5°C

Sample	$M_w / 10^5$	$\langle S^2 \rangle_z / 10^2$ nm^2
F33-1	106	29.7
F33-2	75.0	20.2
F33-3	50.5	13.6
F33-4	35.5	9.21
F33-6	21.8	5.21
F33-7	12.2	2.43
F33-9	8.03	1.39

Figure III-7 shows the molecular weight dependence of $\langle S^2 \rangle_z$ for the polymacromonomer F15 in cyclohexane at the Θ point (34.5°C). The curve has a slope 1.1 for $M_w < 1\times10^6$ and 1.0 for $M_w > 2\times10^6$. A similar graph for the polymacromonomer F33 in the same solvent is displayed in Figure III-8. The slope of the curve decreases from 1.4 to 1.0 with increasing M_w. These non-Gaussian behaviors show unmistakable semiflexibility of the polymacromonomers.

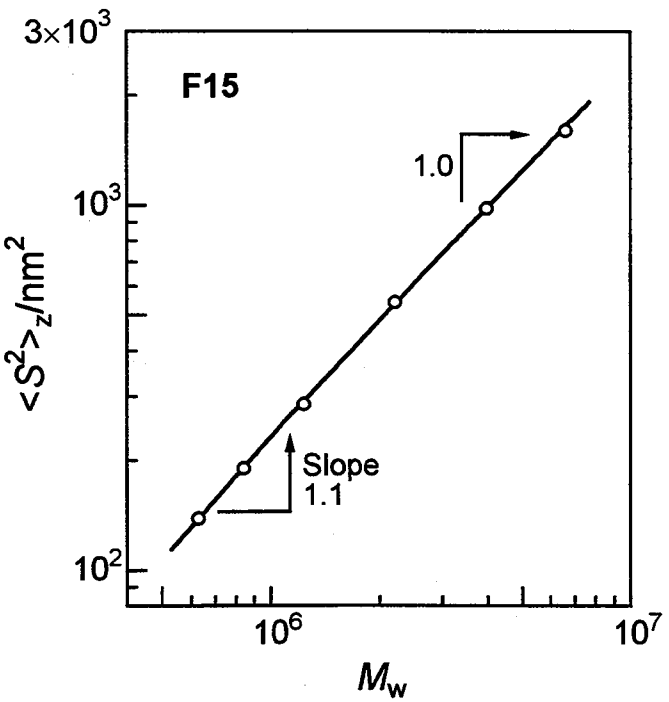

Figure III-7. Molecular weight dependence of $\langle S^2 \rangle_z$ for the polymacromonomer F15 in cyclohexane at 34.5°C. The curve represents eq III-1 for the unperturbed wormlike chain with λ^{-1} = 9.5 nm and M_L = 6200 nm^{-1} (see Section III. 3).

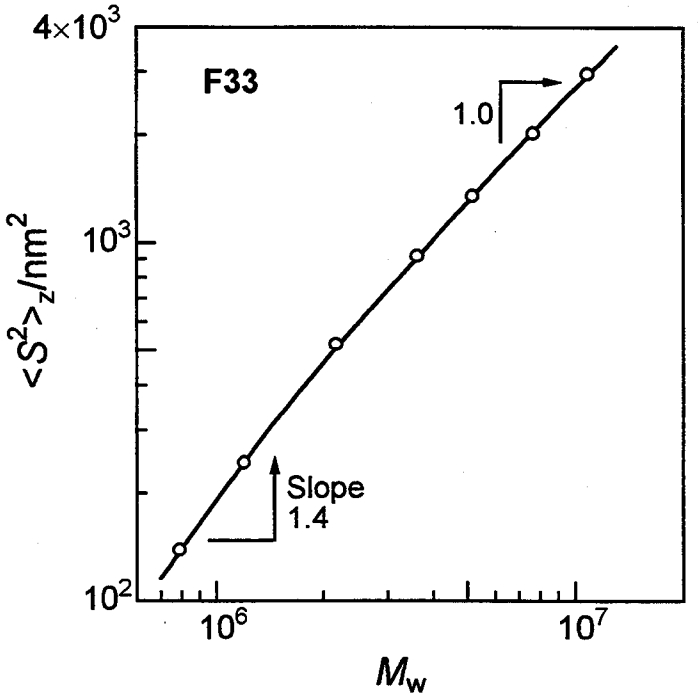

Figure III-8. Molecular weight dependence of $\langle S^2 \rangle_z$ for the polymacromonomer F33 in cyclohexane at 34.5°C. The curve represents eq III-1 for the unperturbed wormlike chain with λ^{-1} = 22 nm and M_L = 13000 nm^{-1} (see Section III. 3).

III. 3 Discussion

III. 3. 1 Analysis of $\langle S^2 \rangle_z$ Data at the Θ Temperature

If our polymacromonomers in cyclohexane is modeled by the wormlike chain,[1] its $\langle S^2 \rangle$ in the unperturbed state, i.e., $\langle S^2 \rangle_0$, may be expressed by[4]

$$\lambda^2 \langle S^2 \rangle_0 = \frac{\lambda L}{6} - \frac{1}{4} + \frac{1}{4\lambda L} - \frac{1}{8(\lambda L)^2}\left[1 - \exp(-2\lambda L)\right] \qquad \text{(III-1)}$$

Here, λ^{-1} is the Kuhn segment length and L is the contour length of the main chain related to the molecular weight M by $L = M/M_L$, with M_L being the molar mass per unit contour length. According to Murakami et al.,[5] eq III-1 can be approximated by

$$\left(\frac{M}{\langle S^2 \rangle_0}\right)^{1/2} = (6\lambda M_L)^{1/2}\left(1 + \frac{3M_L}{4\lambda M}\right) \qquad \text{(III-2)}$$

with the maximum error from exact value being 1% for $\lambda L > 2$. Equation III-2 indicates that $(M/\langle S^2 \rangle_0)^{1/2}$ plotted against M^{-1} (for $M > 2M_L\lambda^{-1}$) should give a straight line whose intercept and slope allow the two parameters λ^{-1} and M_L to be evaluated.

Figure III-9 shows this plot constructed from the $\langle S^2 \rangle_z$ data for the polymacromonomers F15 (panel a) and F33 (panel b) in cyclohexane at the Θ temperature. As expected, the data points for each polymacromonomer follow a straight line. The values of λ^{-1} and M_L evaluated are summarized in Table III-5. The curves in Figures III-7 and III-8 actually represent the theoretical values calculated from eq III-1 with these parameters. Their fits to the data points for both F15 and F33 are excellent. The λ^{-1} value of 22 nm for F33 in Table III-5 shows a considerable stiffness of the polymer, but it is not as large as that (89 nm) reported for the polymacromonomer consisting

of the PMMA backbone and 28 styrene side-chain residues in toluene.[6-8]

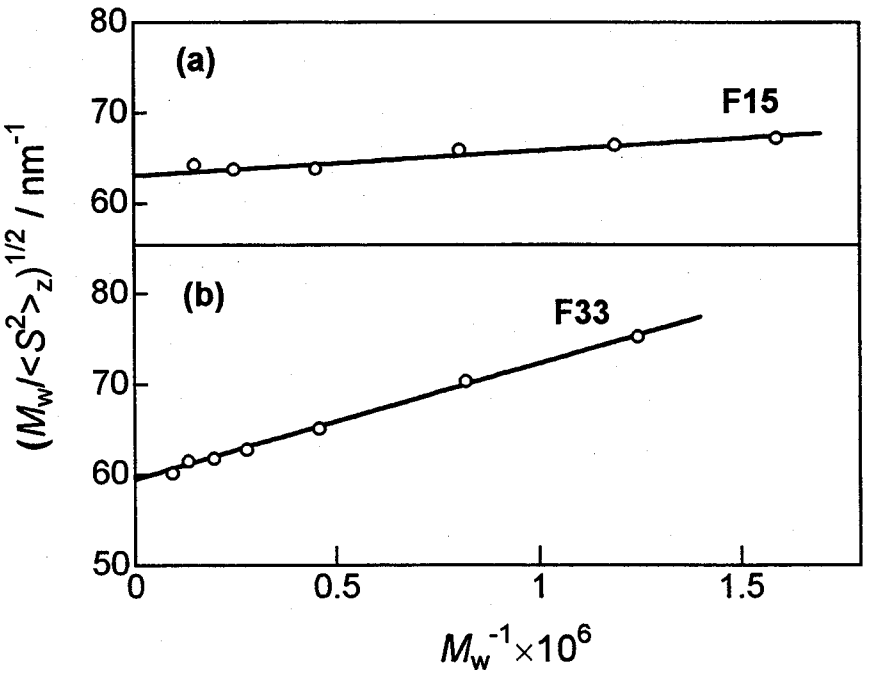

Figure III-9. Plots of $(M_w/<S^2>_z)^{1/2}$ vs. M_w^{-1} for the polymacromonomers F15 (panel a) and F33 (panel b) in cyclohexane at the Θ temperature.

Table III-5. Wormlike-Chain Parameters for the Polymacromonomers F15 and F33 in Cyclohexane at the Θ temperature

Polymer	Θ / °C	λ^{-1} / nm	M_L / 10^3 nm^{-1}
F15	34.5±1	9.5±0.5	6.2±0.2
F33	34.5±2	22 ±1	13.0±0.3

In the above analysis, we ignored possible effects of chain thickness and chain ends on $\langle S^2 \rangle_0$; note that the latter effect may arise if side chains near the ends of the main chain are more or less oriented to the direction of the main-chain contour to apparently increase the contour length (see Figure V-3). We examined these effects by evaluating the mean-square radius of gyration $\langle S^2 \rangle_{0,t}$ of a wormlike polymacromonomer whose side chains are flexible (but yet wormlike) and linked to the stiffer backbone by completely flexible joints (see Appendix A). The resulting expression is the sum of $\langle S^2 \rangle_0$ of the backbone (i.e., eq. III-1) and the contribution $\langle S^2 \rangle_{0,s}$ from the side chains, i.e.,

$$\langle S^2 \rangle_{0,t} = \langle S^2 \rangle_0 + \langle S^2 \rangle_{0,s} \tag{III-3}$$

$$\begin{aligned} \langle S^2 \rangle_{0,s} = \frac{N-1}{N}\left\{\frac{L_s}{2\lambda_s} - \frac{1}{2\lambda_s^2} + \frac{1}{4\lambda_s^3 L_s}\left[1-\exp(-2\lambda_s L_s)\right]\right\} \\ + \frac{1}{N}\left\{\frac{L_s}{6\lambda_s} - \frac{1}{4\lambda_s^2} + \frac{1}{4\lambda_s^3 L_s} - \frac{1}{8\lambda_s^4 L_s^2}\left[1-\exp(-2\lambda_s L_s)\right]\right\} \end{aligned} \tag{III-4}$$

In eq III-4, λ_s and L_s denote the values of λ and L, respectively, for each side chain and N is the number of side chains in the polymacromonomer (i.e., the degree of polymerization of the main chain); note that $L_s = M_s/M_{L,s}$, with M_s and $M_{L,s}$ being the molecular weight and linear mass density of each side chain.

The $\langle S^2 \rangle_{0,s}$ computed as a function of the molecular weight M of the polymacromonomer F15 with $M_s = 1.53\times10^3$ (see Table II-1 in Chapter II),

λ_S^{-1} = 2.0 nm, and $M_{L,S}$ = 390 nm^{-1} (the wormlike-chain parameters for linear PS[9]) was about 2.4 nm^2, almost regardless of M above 1×10^5, and its contribution to $<S^2>_{0,t}$ was 1.6% for $M = 6.6\times10^5$, the lowest molecular weight with which we are concerned here. Similar calculation for the polymacromonomer F33 with $M_S = 3.44\times10^3$ gave $<S^2>_{0,S}$ of about 7 nm^2 ($M > 2\times10^5$), whose contribution to $<S^2>_{0,t}$ was 2.9% for $M = 1.22\times10^6$ and 5% even for $M = 8.0\times10^5$. Since those contributions are hardly beyond experimental errors of $<S^2>_Z$, we convince ourselves that the present $<S^2>_Z$ data are essentially free from the above-mentioned effects of side chains and that the analysis based on eq III-1 introduces no significant error in the wormlike-chain parameters.

III. 3. 2 Molecular Characteristics

The M_L value of 6200 nm^{-1} for the polymacromonomer F15 (Table III-5) with the molar mass (1650 g mol^{-1}) of the macromonomer (see Table II-2 in Chapter II) yields a value of 0.27 nm for the monomeric length h along the main-chain contour. Essentially the same h value is obtained for F33 whose macromonomer has a molar mass of 3560 g mol^{-1}. This suggests that the local conformation of the PS backbone is insensitive to side chain length. It is of interest to note that the h values of about 0.27 nm are close to that (0.25 nm) calculated on the assumption that the PS backbone assumes the *all-trans* conformation. The slightly larger experimental estimate becomes very close to the *all-trans* value if M_L is corrected for the polydispersity (M_Z/M_W = 1.06)

of polymacromonomer F15 samples (F15-2 through F15-6) in the analysis of $\langle S^2 \rangle_z$ by replacing L in eq III-1 with the z-average L ($= M_z/M_L$); note that for $M > 6\times10^5$, $\langle S^2 \rangle_0$ is determined substantially by the first two leading terms of eq III-1. A similar correction for the polymacromonomer F33 should also lead to an h closer to the *all-trans* value.

While the contour length per main chain residue is insensitive to the side chain length, λ^{-1} is an increasing function of it. The λ^{-1} value of 22 nm for the F33 polymer in cyclohexane at 34.5°C is more than twice that for F15 in the same solvent and one order of magnitude lager than that (2 nm) for the linear PS molecule[9] modeled by the wormlike chain; note that linear PS is better modeled by the helical wormlike chain and that λ^{-1} (the stiffness parameter) in this model is 2.1 – 2.7 nm.[10-14] The pronounced effect of side chain length on λ^{-1}, observed here, is in line with what was found by Wintermantel et al.[7] for polymacromonomers consisting of the PMMA backbone and PS side chains in toluene, a good solvent. Our new finding is that even in the absence of excluded-volume interaction (in the conventional framework of polymer solution theory[15]), the polymacromonomer backbone is remarkably stiffened by the high segment density.

Appendix A. Radius of Gyration of a Wormlike Polymacromonomer

In this appendix, we derive eqs III-3 and III-4 for $\langle S^2 \rangle_{0,t}$ of a wormlike polymacromonomer whose N flexible side chains each having contour length L_S are linked to a stiffer backbone of contour length L by completely flexible

joints. Denoting the mean-square distance between two contour points r and r' on the polymer by $\langle R^2(r, r')\rangle$, we have

$$\langle S^2\rangle_{0,t} = \frac{1}{L_t^2} \sum\sum_{(all\ combinations)} \left\langle R^2(r,r')\right\rangle \tag{A-1}$$

where the *total* contour length L_t is given by

$$L_t = L + NL_s \tag{A-2}$$

The mean-square distance can be divided into four cases depending on whether the points r and r' are on the main chain or ith side chain (i = 1, 2, 3, ..., N), as schematically shown in Figure A-1, and $\langle S^2\rangle_{0,t}$ is written

$$\langle S^2\rangle_{0,t} = \frac{1}{L_t^2}(I_1 + I_2 + I_3 + I_4) \tag{A-3}$$

where

$$I_1 = \int_0^L \mathrm{d}r \int_r^L \mathrm{d}r' \left\langle R^2(r,r')\right\rangle_m \tag{A-4}$$

$$I_2 = \sum_{i=1}^{N} \int_0^{L_s} \mathrm{d}r_i \int_{r_i}^{L_s} \mathrm{d}r_i' \left\langle R^2(r_i,r_i')\right\rangle_s \tag{A-5}$$

$$\begin{aligned} I_3 &= \sum_{i=1}^{N} \int_0^L \mathrm{d}r \int_0^{L_s} \mathrm{d}r_i' \left\langle R^2(r,r_i')\right\rangle \\ &= \sum_{i=1}^{N} \int_0^L \mathrm{d}r \int_0^{L_s} \mathrm{d}r_i' \left(\left\langle R^2(r,r_{i0}')\right\rangle_m + \left\langle R^2(r_{i0}',r_i')\right\rangle_s \right) \end{aligned} \tag{A-6}$$

$$I_4 = \sum_{i=1}^{N-1} \sum_{j=i+1}^{N} \int_0^{L_s} \mathrm{d}r_i \int_0^{L_s} \mathrm{d}r_j' \left\langle R^2(r_i, r_j') \right\rangle$$

$$= \sum_{i=1}^{N-1} \sum_{j=i+1}^{N} \int_0^{L_s} \mathrm{d}r_i \int_0^{L_s} \mathrm{d}r_j' \left(\left\langle R^2(r_i, r_{i0}) \right\rangle_s + \left\langle R^2(r_{i0}, r_{j0}') \right\rangle_m + \left\langle R^2(r_{j0}', r_j') \right\rangle_s \right)$$

(A-7)

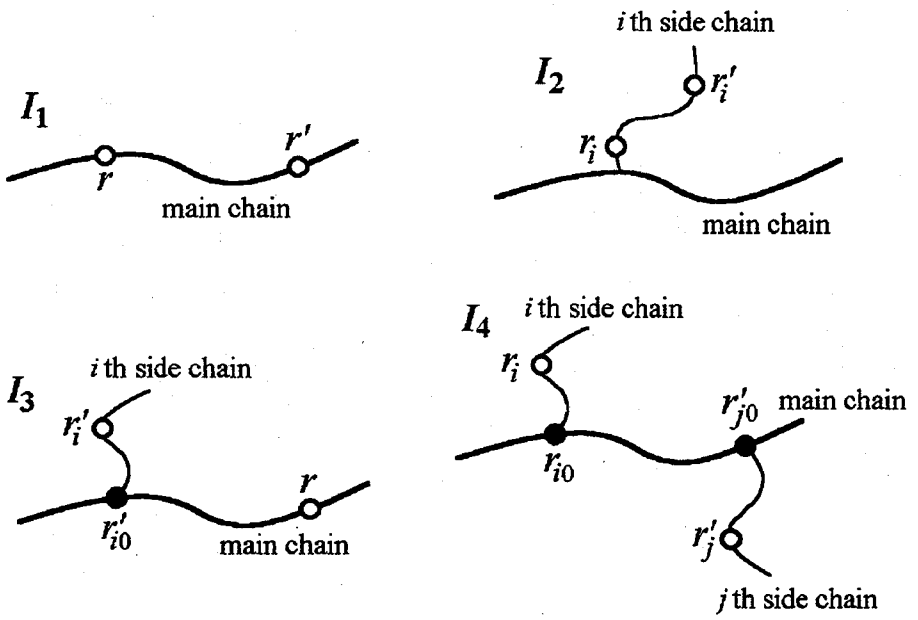

Figure A-1. Schematic diagrams for the four terms in eq A-3.

The subscript m (or s) attached to $\langle R^2(r, r') \rangle$ signifies that both r and r' are located on the main chain (or on the same side chain under consideration), and the second equality in eq A-6 or A-7 is due to the present model that each side chain is linked to the main chain by a completely flexible joint (at the position indicated by a filled circle in Figure A-1).

Now, $\langle R^2(r, r')\rangle_m$ and $\langle R^2(r, r')\rangle_s$ are given by[16]

$$\left\langle R^2(r,r')\right\rangle_m = \frac{|r'-r|}{\lambda} - \frac{1}{2\lambda^2}\left[1-\exp\left(-2\lambda|r'-r|\right)\right] \qquad \text{(A-8)}$$

$$\left\langle R^2(r,r')\right\rangle_s = \frac{|r'-r|}{\lambda_s} - \frac{1}{2\lambda_s^2}\left[1-\exp\left(-2\lambda_s|r'-r|\right)\right] \qquad \text{(A-9)}$$

with λ^{-1} and λ_s^{-1} being the Kuhn segment length of the main chain and that of each side chain, respectively. Substitution of these expressions into eqs A-4 – A-7, followed by integration and summation, gives eq III-3 with eq III-4 in the text. Interestingly, eq III-3 in the coil limit reduces to the familiar Zimm-Stockmayer equation[17] for Gaussian stars of N arms if L is set equal to zero.

References

1. O. Kratky and G. Porod, *Rec. Trav. Chim.*, **68**, 1106 (1949).
2. See, for example, Y. Nakamura, T. Norisuye, and A. Teramoto, *Macromolecules*, **24**, 4904 (1991).
3. Y. Takeo, M. S. Thesis, Osaka University, 1997.
4. H. Benoit and P. Doty, *J. Phys. Chem.*, **57**, 958 (1953).
5. H. Murakami, T. Norisuye, and H. Fujita, *Macromolecules*, **13**, 345 (1980).
6. M. Wintermantel, M. Schmidt, Y. Tsukahara, K. Kajiwara, and S. Kohjiya, *Macromol. Rapid Commun.*, **15**, 279 (1994).
7. M. Wintermantel, M. Gerle, K. Fischer, M. Schmidt, I. Wataoka, H. Urakawa, K. Kajiwara, and Y. Tsukahara, *Macromolecules*, **29**, 978 (1996).
8. N. Nemoto, M. Nagai, A. Koike, and S. Okada, *Macromolecules*, **28**, 3854 (1995).
9. T. Norisuye and H. Fujita, *Polym. J.*, **14**, 143 (1982).
10. H. Yamakawa, *Helical Wormlike Chains in Polymer Solutions*, Springer, Berlin, 1997.
11. Y. Einaga, H. Koyama, T. Konishi, and H. Yamakawa, *Macromolecules*, **22**, 3419 (1989).
12. T. Konishi, T. Yoshizaki, T. Saito, Y. Einaga, and H. Yamakawa, *Macromolecules*, **23**, 290 (1990).
13. T. Konishi, T. Yoshizaki, and H. Yamakawa, *Macromolecules*, **24**, 5614 (1991).
14. T. Yamada, T. Yoshizaki, and H. Yamakawa, *Macromolecules*, **25**, 377 (1992).
15. H. Yamakawa, *Modern Theory of Polymer Solutions*, Harper & Row, New York, 1971.
16. G. Porod, *J. Polym. Sci.* **10**, 157 (1953).
17. B. H. Zimm and W. H. Stockmayer, *J. Chem. Phys.*, **17**, 1301 (1949).

Chapter IV Chain Dimensions and Chain Stiffness in Non-ideal Solvents: Solvent Effect

IV. 1 Introduction

In the preceding chapter, we found from analyses of measured z-average radii of gyration $\langle S^2 \rangle_z^{1/2}$ for the polymacromonomers F15 and F33 in cyclohexane at the Θ temperature that the chain stiffness expressed in terms of the Kuhn segment length λ^{-1} in the wormlike chain model[1] is almost one order of magnitude higher than that of the linear polystyrene (PS) molecule at the Θ point. This indicates that the high segment density around the polymacromonomer main chain remarkably stiffens the backbone even in the absence of excluded-volume interaction. It is thus intriguing to see whether the stiffness changes when the solvent condition is varied from the Θ state to a good solvent. No such work is yet done on polymacromonomer solutions.

In this chapter, $\langle S^2 \rangle_z$ data for F15 and F33 samples in cyclohexane at temperatures other than Θ and in toluene at 15°C are presented as functions of weight-average molecular weight M_w and analyzed on the basis of the wormlike chain.[1] Excluded volume effects on $\langle S^2 \rangle_z$ are taken into account in the framework of the quasi-two-parameter theory,[2-4] since, as shown below, they are not negligible at high molecular weights.

IV. 2 Results

IV. 2. 1 Cyclohexane Solutions near the Θ Temperature

Figure IV-1 illustrates the plots of $(Kc/R_\theta)_{c=0}^{1/2}$ vs. $\sin^2(\theta/2)$ for the sample F15-1 in cyclohexane at the indicated temperatures T, where K, c, and R_θ denote the optical constant, the polymer mass concentration, and the excess reduced scattering intensity at scattering angle θ, respectively. The curves fitting the plotted points at the respective T converge to a common intercept within experimental error. The values of $\langle S^2 \rangle_z$ evaluated from their initial

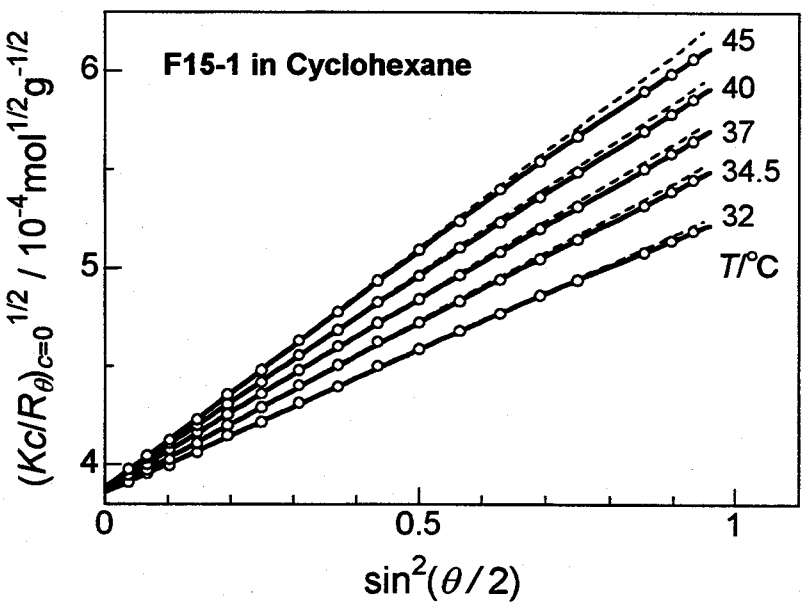

Figure IV-1. Angular dependence of $(Kc/R_\theta)_{c=0}^{1/2}$ for sample F15-1 in cyclohexane at indicated temperatures. Dashed lines, initial slopes; wavelength of incident light, 436 nm.

slopes (the dashed lines) are plotted against T in Figure IV-2, along with those for other 5 samples. The T-dependence of $\langle S^2 \rangle_z$ for every sample is much weaker than that for linear PS with the same molecular weight in cyclohexane.[5] Similar plots for polymacromonomer F33 samples in cyclohexane are displayed in Figure IV-3. Their T-dependence is slightly weaker than that for F15 (compare at the same molecular weight). All the values of $\langle S^2 \rangle_z$ for F15 and F33 are summarized in Tables IV-1 and IV-2, respectively, in which the M_w value only for 546 nm at 34.5°C is given for each sample, since it agreed with those obtained for the two wavelengths at different temperatures within $\pm 1\%$.

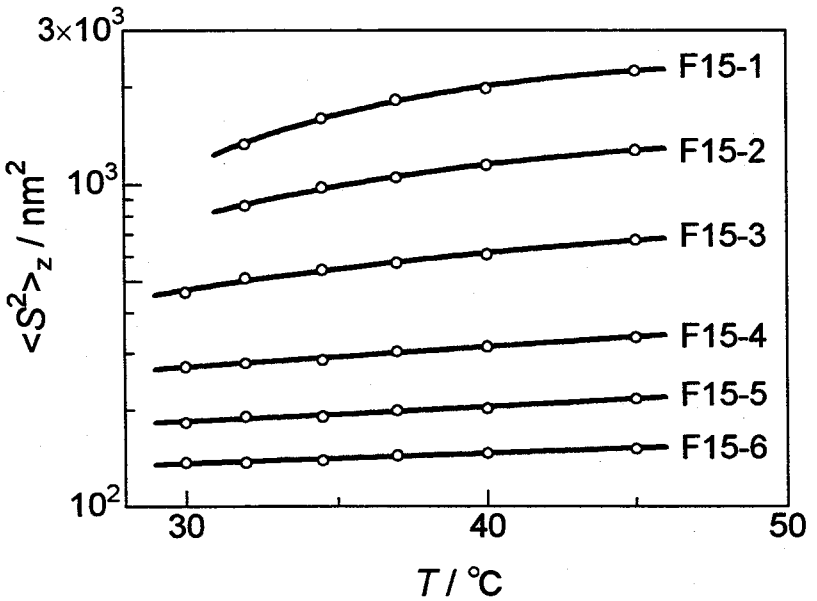

Figure IV-2. Temperature dependence of $\langle S^2 \rangle_z$ for the indicated F15 samples in cyclohexane.

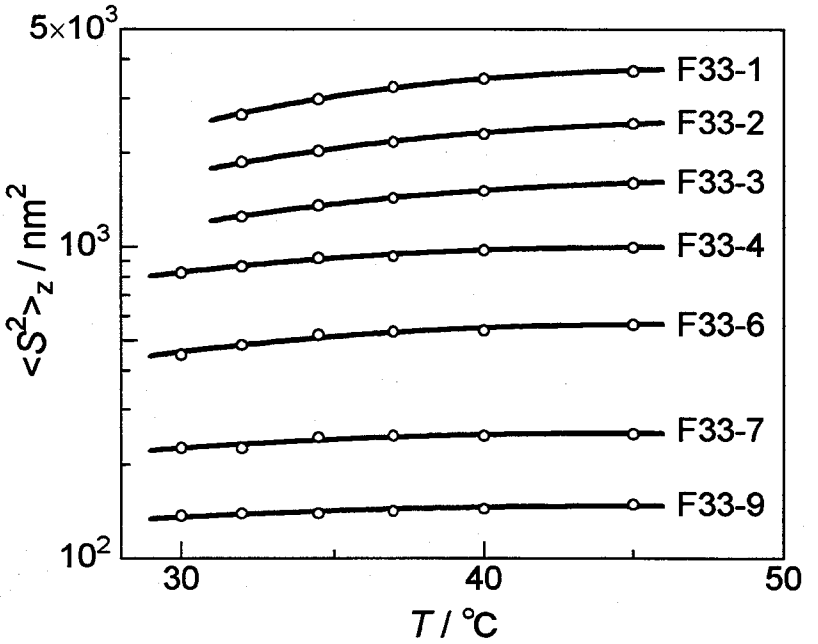

Figure IV-3. Temperature dependence of $\langle S^2 \rangle_z$ for the indicated F33 samples in cyclohexane.

Table IV-1. Values of $\langle S^2 \rangle_z$ for Polymacromonomer F15 Samples in Cyclohexane at Different Temperatures

		$\langle S^2 \rangle_z / 10^2 nm^2$					
Sample	$M_w / 10^5$ [a]	30°C	32°C	34.5°C	37°C	40°C	45°C
F15-1	66.1		13.3	16.0	18.2	19.8	22.5
F15-2	39.8		8.58	9.80	10.5	11.5	12.7
F15-3	22.1	4.62	5.11	5.43	5.71	6.05	6.71
F15-4	12.4	2.72	2.79	2.86	3.03	3.13	3.35
F15-5	8.41	1.82	1.90	1.90	1.99	2.02	2.16
F15-6	6.29	1.37	1.37	1.39	1.44	1.46	1.51

[a] Determined at 34.5°C and 546 nm

Table IV-2. Values of $\langle S^2 \rangle_z$ for Polymacromonomer F33 Samples in Cyclohexane at Different Temperatures

		$\langle S^2 \rangle_z / 10^2 nm^2$					
Sample	$M_w / 10^5$ [a]	30°C	32°C	34.5°C	37°C	40°C	45°C
F33-1	106		26.5	29.7	32.5	34.6	36.7
F33-2	75.0		18.6	20.2	21.6	23.0	24.9
F33-3	50.5		12.5	13.6	14.3	15.0	16.0
F33-4	35.5	8.21	8.63	9.21	9.33	9.71	9.90
F33-6	21.8	4.51	4.83	5.21	5.34	5.38	5.62
F33-7	12.2	2.25	2.26	2.43	2.46	2.46	2.50
F33-9	8.03	1.37	1.39	1.39	1.42	1.44	1.49

[a] Determined at 34.5°C and 546 nm

IV. 2. 2 Toluene Solutions

Figure IV-4 shows the light scattering envelopes for sample F33-1 in toluene at 15°C. The value of $\langle S^2 \rangle_z$ for this sample was evaluated from the dashed line tangentially fitting the filled circles in panel (a). The numerical data of M_w, A_2 (the second virial coefficient), and $\langle S^2 \rangle_z$ obtained for toluene solutions of the F15 and F33 polymers are all summarized in Tables IV-3 and IV-4, respectively. We note that the M_w values determined in toluene and cyclohexane agree with each other within $\pm 1.7\%$.

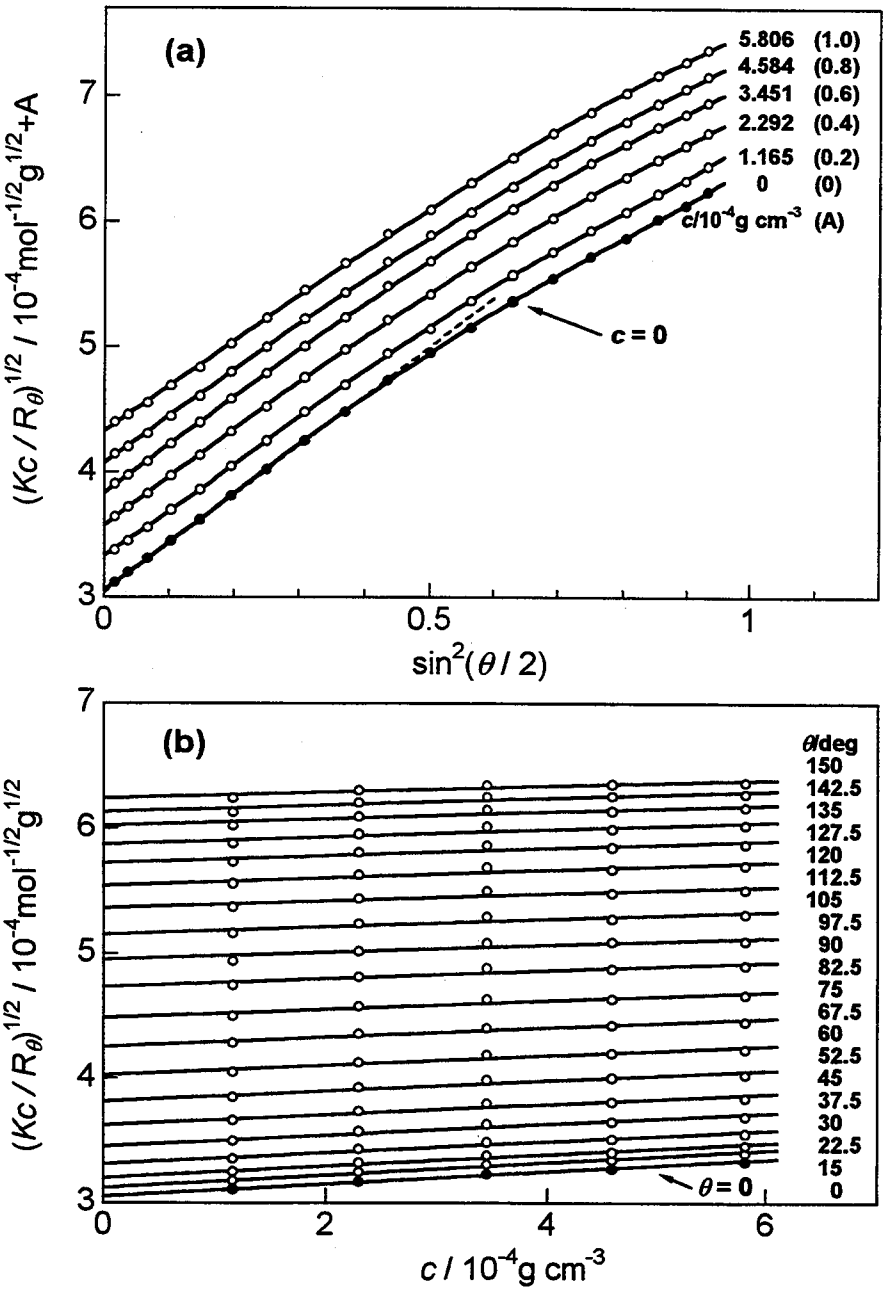

Figure IV-4. Plots of $(Kc/R_\theta)^{1/2}$ vs. $\sin^2(\theta/2)$ at indicated c (a) and $(Kc/R_\theta)^{1/2}$ vs. c at fixed scattering angles (b) for sample F33-1 in toluene at 15°C. For clarity, the ordinate values of $(Kc/R_\theta)^{1/2}$ in panel (a) are shifted by A. Wavelength of incident light, 546 nm; filled circles, extrapolated values.

Table IV-3. Results from Light Scattering Measurements on Polymacromonomer F15 Samples in Toluene at 15°C

Sample	M_w / 10^5	A_2 / 10^{-5}cm^{3}mol g^{-2}	$\langle S^2 \rangle_z$ / 10^2nm^2
F15-1	64.7	2.6	40.1
F15-2	40.4	2.9	22.8
F15-3	22.5	2.6	11.2
F15-4	12.3	3.6	5.24
F15-5	8.22	4.0	3.35
F15-6	6.09	4.3	2.31
F15-7	3.81	5.3	1.21
F15-8	2.52	6.6	
F15-9	1.75	8.2	
F15-10	1.23	8.3	
F15-11	0.614	12.2	
F15-12	0.474	16.1	
F15-13	0.260	30.8	
F15-14	0.108	53.0	
F15-15	0.0514	94.6	

Table IV-4. Results from Light Scattering Measurements on Polymacromonomer F33 Samples in Toluene at 15°C

Sample	$M_w / 10^5$	$A_2 / 10^{-5}$cm^{3}mol g^{-2}	$\langle S^2 \rangle_z / 10^2$nm^2
F33-1	108	1.5	64.0
F33-2	76.5	1.5	42.1
F33-3	51.7	1.6	26.1
F33-4	36.2	1.8	16.0
F33-5	28.9	1.6	11.4
F33-6	22.0	2.2	8.01
F33-7	12.0	2.2	3.39
F33-8	8.73	2.5	2.10
F33-9	7.90	3.0	1.85
F33-10	3.84	4.7	
F33-13	1.28	10.7	
F33-14	0.543	24.7	

The molecular weight dependence of A_2 for F15 and F33 in toluene at 15°C is illustrated in Figure IV-5. The curves for both polymers have a very large negative slope of –0.80 at low M_w and a small (or usual) negative slope of about –0.20 at high M_w. For $M_w > 6\times10^5$, the values of A_2 are all on the order 10^{-5} mol cm^3g^{-2}, but those for the F33 polymer are systematically smaller.

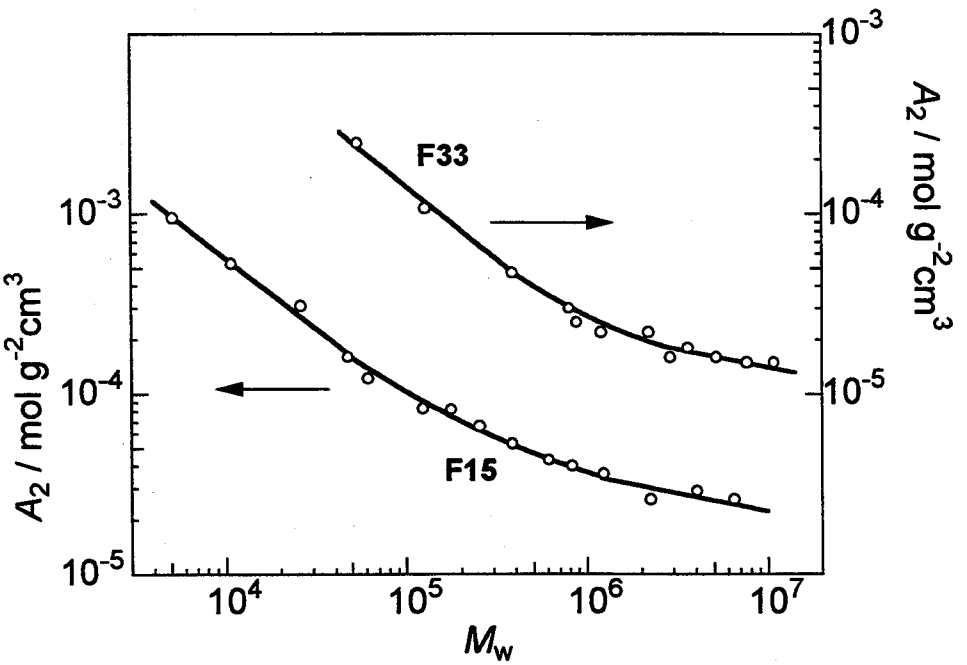

Figure IV-5. Molecular weight dependence of A_2 for the polymacromonomers F15 and F33 in toluene at 15°C.

Figure IV-6 shows the molecular weight dependence of $\langle S^2 \rangle_z$ for the polymacromonomer F15 in toluene at 15°C, along with that in cyclohexane at 34.5°C reproduced for comparison from Figure III-7 in Chapter III. The indicated solid and dashed lines are explained in the next section. We here note that the curve for toluene solutions has a slope 1.4 for $M_w < 8\times10^5$ and 1.2 for $M_w > 2\times10^6$. Similar plots of log $\langle S^2 \rangle_z$ vs. log M_w for the polymacromonomer F33 in the two solvents are displayed in Figure IV-7. The slope of the solid curve for toluene solutions decreases from 1.6 to 1.2 with increasing M_w.

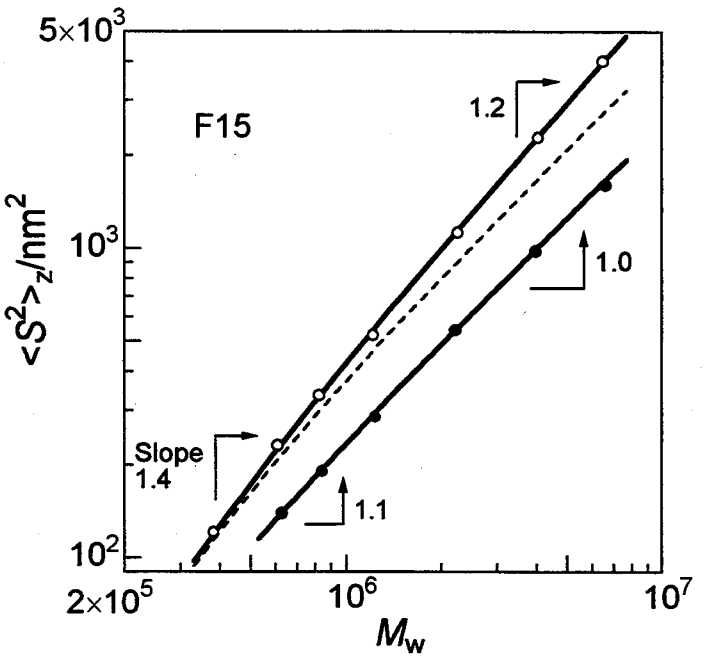

Figure IV-6. Molecular weight dependence of $\langle S^2 \rangle_z$ for the polymacromonomer F15 in toluene at 15°C (○) and in cyclohexane at 34.5°C (●). Solid curves, theoretical values calculated from eqs III-1 and IV-1 with the parameters in Table IV-5; dashed line, theoretical values for $B = 0$.

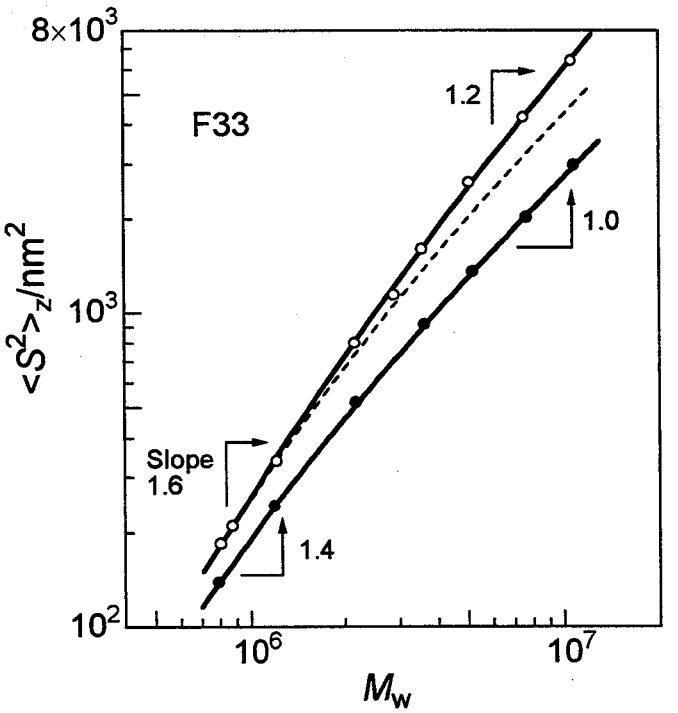

Figure IV-7. Molecular weight dependence of $\langle S^2 \rangle_z$ for the polymacromonomer F33 in toluene at 15°C (○) and in cyclohexane at 34.5°C (●). Solid curves, theoretical values calculated from eqs III-1 and IV-1 with the parameters in Table IV-5; dashed line, theoretical values for $B = 0$.

IV. 3 Discussion

IV. 3. 1 Data Analysis

Polymacromonomers F15 and F33 in Cyclohexane

Figure IV-8 shows the plot of $(M_w/\langle S^2 \rangle_z)^{1/2}$ vs. M_w^{-1} constructed from our $\langle S^2 \rangle_z$ data for the F33 polymer in cyclohexane at 45°C according to eq

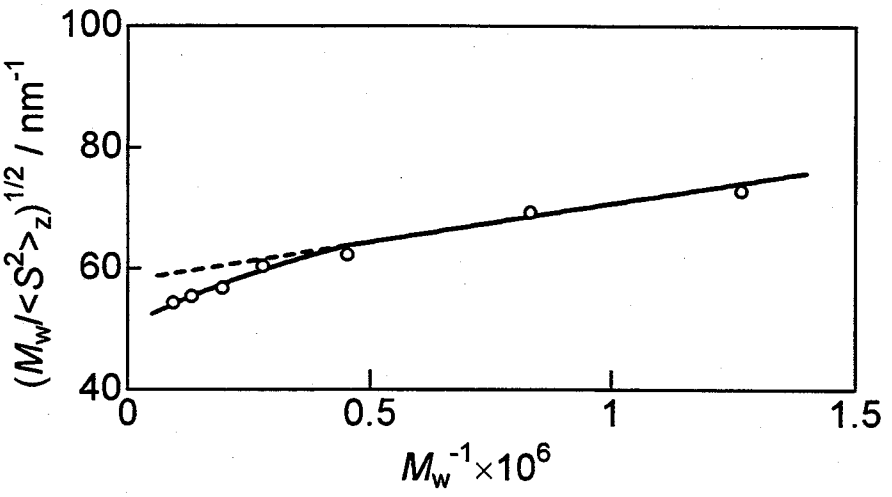

Figure IV-8. Plots of $(M_w/<S^2>_z)^{1/2}$ vs. M_w^{-1} for the polymacromonomer F33 in cyclohexane at 45°C.

III-2. The plotted points do not obey the linear relation of $(M_w/<S^2>_z)^{1/2}$ vs. M_w^{-1}. The pronounced downward deviations from the dashed line may be ascribed to excluded-volume effects on $<S^2>_z$ at this temperature. Similar deviations were observed at other temperatures and also for the F15 polymer. In the following, we analyze $<S^2>_z$ data for the F15 and F33 polymers in cyclohexane near the Θ temperature with the aid of the quasi-two-parameter (QTP) theory[2-4] for wormlike[1] or helical wormlike[2] bead chains. As mentioned in Chapter I, this theory allows an accurate description of $<S^2>$ for linear flexible and semiflexible polymers[2,6-10] over a broad range of molecular weight.

The radius expansion factor α_s [$\equiv (\langle S^2\rangle / \langle S^2\rangle_0)^{1/2}$] in the QTP scheme[2-4] is expressed by

$$\alpha_s^2 = \left[1+10\tilde{z}+\left(\frac{70\pi}{9}+\frac{10}{3}\right)\tilde{z}^2+8\pi^{3/2}\tilde{z}^3\right]^{2/15} \times[0.933+0.067\exp(-0.85\tilde{z}-1.39\tilde{z}^2)] \qquad \text{(IV-1)}$$

if the Domb-Barrett function[11] is adopted. Here, $\tilde{z}$ is the scaled excluded-volume parameter defined by

$$\tilde{z} = \frac{3}{4}K(\lambda L)z \qquad \text{(IV-2)}$$

with

$$z = \left(\frac{3}{2\pi}\right)^{3/2}(\lambda B)(\lambda L)^{1/2} \qquad \text{(IV-3)}$$

and

$$K(\lambda L) = \frac{4}{3}-2.711(\lambda L)^{-1/2}+\frac{7}{6}(\lambda L)^{-1} \quad \text{for } \lambda L > 6$$

$$= (\lambda L)^{-1/2}\exp[-6.611(\lambda L)^{-1}+0.9198+0.03516\lambda L] \quad \text{for } \lambda L \le 6 \qquad \text{(IV-4)}$$

In eq IV-3, z is the conventional excluded-volume parameter and B is the

excluded-volume strength defined for the wormlike chain by

$$B = \beta / a^2 \qquad \text{(IV-5)}$$

with β and a being the binary cluster integral representing the interaction between a pair of beads and the bead spacing, respectively. In our case, one bead must contain a number of main-chain residues but need not be specified.

Equations IV-1 through IV-5 indicate that B needs to be known (in addition to λ^{-1} and the molar mass per unit contour length M_L) in order to evaluate theoretical α_s^2 and hence theoretical $\langle S^2 \rangle$ in a perturbed state. A curve fitting procedure was employed for the determination of the parameters, but M_L at any T was assumed to be the same as that in cyclohexane at 34.5°C; we note that the three parameters could not uniquely be determined from the $\langle S^2 \rangle_z$ data because of the correlation between λ^{-1} and B in the fitting in the molecular weight range studied here. The parameters obtained for the two polymacromonomers are summarized in Table IV-5, in which those at 34.5°C are the reproductions from Table III-5.

Figure IV-9 compares the experimental $\langle S^2 \rangle_z / M_w$ for the F15 polymer in cyclohexane at the indicated temperatures with the theoretical solid lines calculated from eqs III-1 and IV-1 with the parameters in Table IV-5. The agreement is satisfactory at any temperatures. The dashed line at each T refers to the unperturbed state (i.e., $B = 0$). Excluded volume effects are appreciable at any temperatures other than Θ. In particular, at 45°C they

appear over the entire range of M_W studied.

A similar comparison for the polymacromonomer F33 is made in Figure IV-10. The agreement between theory and experiment is as good as that observed above for F15, and excluded-volume effects are less pronounced because the F33 polymer is stiffer than F15 at any T (see Table IV-5).

Table IV-5. Wormlike-Chain Parameters and Excluded-Volume Strength for the Polymacromonomers F15 and F33 in Cyclohexane at Different Temperatures and in Toluene at 15°C

Polymer	Solvent	T / °C	λ^{-1} / nm	M_L / 10^3nm^{-1}	B / nm
F15	Cyclohexane	32	9.4	6.2 [a]	-0.4
F15	Cyclohexane	34.5	9.5	6.2	0
F15	Cyclohexane	37	9.5	6.2 [a]	0.3
F15	Cyclohexane	40	9.6	6.2 [a]	0.6
F15	Cyclohexane	45	9.8	6.2 [a]	1.2
F15	Toluene	15	16	6.2 [a]	4.5
F33	Cyclohexane	32	21	13.0 [a]	-0.4
F33	Cyclohexane	34.5	22	13.0	0
F33	Cyclohexane	37	23	13.0 [a]	0.5
F33	Cyclohexane	40	23	13.0 [a]	1.5
F33	Cyclohexane	45	24	13.0 [a]	2.4
F33	Toluene	15	36	13.0 [a]	18

[a] Assumed

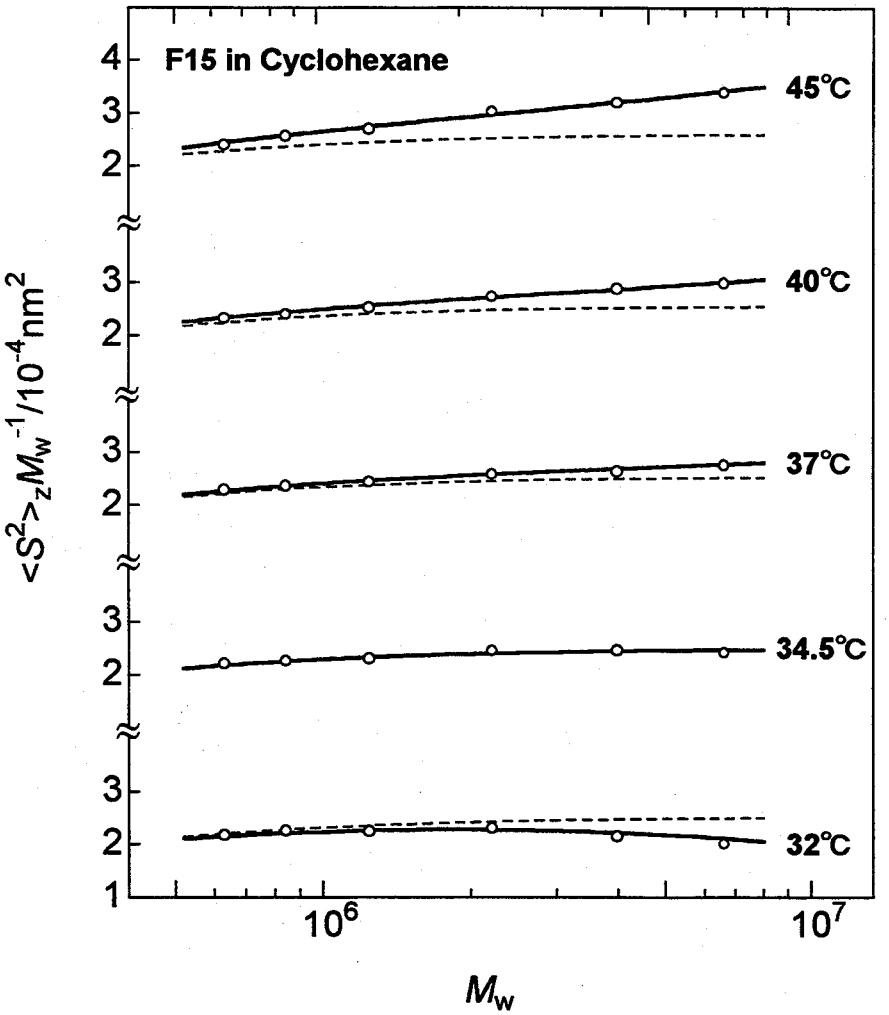

Figure IV-9. Comparison between the measured $<S^2>_z M_w^{-1}$ for the polymacromonomer F15 in cyclohexane at the indicated temperatures and the theoretical values (solid lines) calculated from eqs III-1 and IV-1 with the parameters in Table IV-5. Dashed lines, theoretical values for $B = 0$.

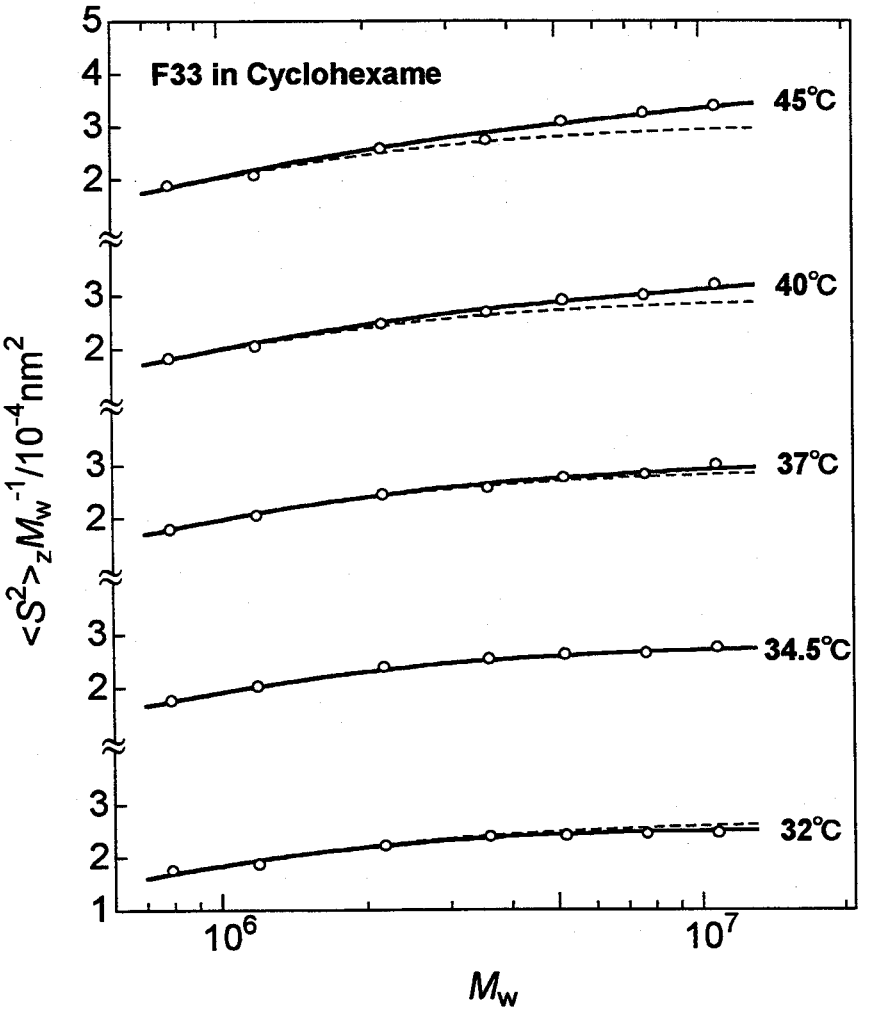

Figure IV-10. Comparison between the measured $<S^2>_z M_w^{-1}$ for the polymacromonomer F33 in cyclohexane at the indicated temperatures and the theoretical values (solid lines) calculated from eqs III-1 and IV-1 with the parameters in Table IV-5. Dashed lines, theoretical values for $B = 0$.

If we rely on the $\langle S^2\rangle_z$ data for $M_w < 3\times10^6$ and analyze them (at the respective T) using eq III-2 for the unperturbed wormlike chain (cf. the dashed line in Figure IV-8), we obtain essentially the same M_L values as 13000nm^{-1} (the value at 34.5°C) and λ^{-1} values indistinguishable from those given in Table IV-5. This finding lends support to the above assumption that M_L of the polymacromonomer in cyclohexane near Θ is essentially independent of T.

Polymacromonomers F15 and F33 in Toluene

The $\langle S^2\rangle_z$ data for the two polymers in toluene do not follow the linear relation (eq III-2) between $(M_w/\langle S^2\rangle_z)^{1/2}$ and M_w^{-1} for unperturbed wormlike chains. Thus their analysis was made in the way used above for cyclohexane solutions near Θ, assuming that M_L for each polymer in toluene is the same as that in cyclohexane at 34.5°C. The parameters thus obtained are included in Table IV-5.

The solid lines drawn for the toluene data in Figures IV-6 and IV-7 represent the theoretical $\langle S^2\rangle$ values calculated from eqs III-1 and IV-1 with the parameters in Table IV-5. They closely fit the unfilled circles for the respective polymacromonomers. The dashed line in either figure again refers to the unperturbed state. Its pronounced downward deviation from the corresponding solid curve substantiates that consideration of excluded-volume effects is important to the experimental estimation of λ^{-1}, at least, for our polymacromonomers in toluene, a good solvent.

IV. 3. 2 Effects of Solvent on Molecular Characteristics

Figures IV-11 and IV-12 illustrate the temperature dependence of λ^{-1} and B, respectively. As the temperature increases, λ^{-1} and B for the polymacromonomers F15 and F33 in cyclohexane gradually increase. This finding suggests that enhancement of side chain – side chain or main chain – side chain repulsion causes the polymer backbone to be stiffened; note that by its definition (i.e., the bending force constant divided by the product of the Boltzmann constant and the absolute temperature T), λ^{-1} may generally be expected to decrease with raising T.

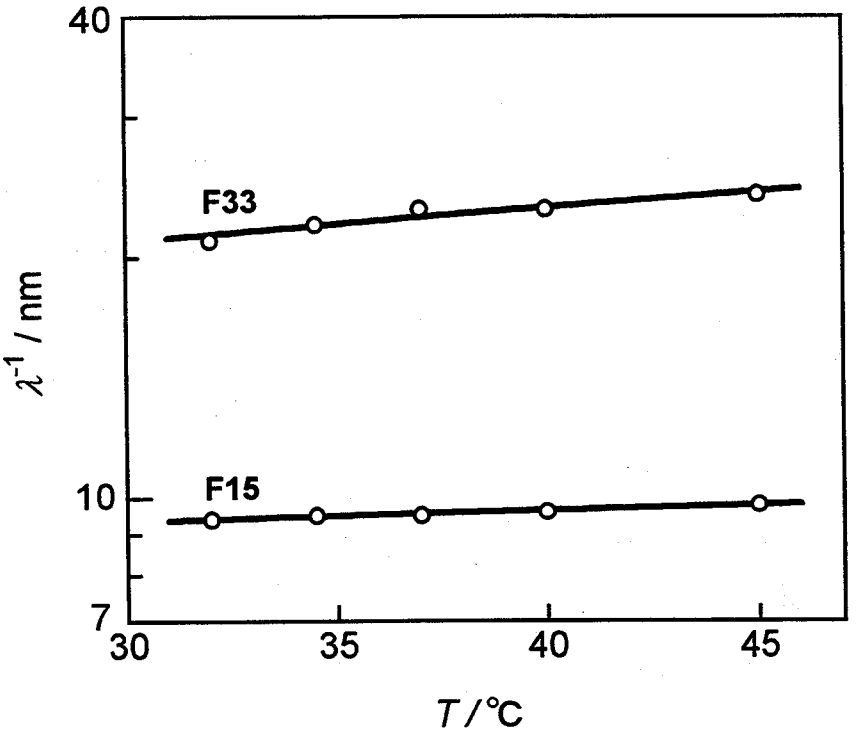

Figure IV-11. Temperature dependence of λ^{-1} for the polymacromonomers F15 and F33 in cyclohexane.

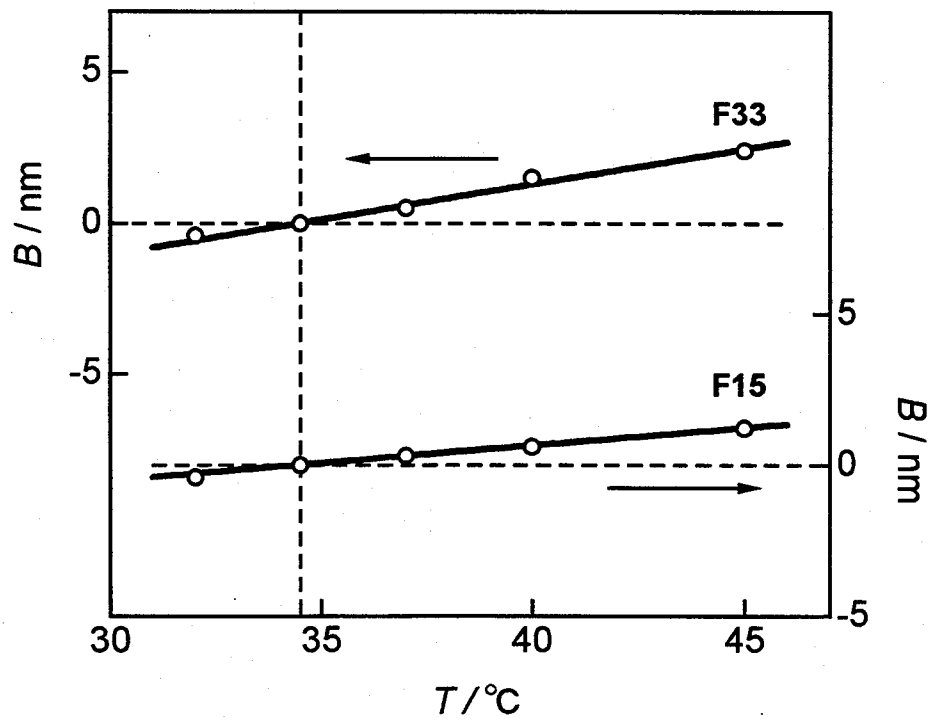

Figure IV-12. Temperature dependence of B for the polymacromonomers F15 and F33 in cyclohexane.

Table IV-5 indeed shows that λ^{-1} and B for both polymers in toluene are much larger than those in cyclohexane near Θ, the increases of λ^{-1} amounting to 1.6 times. This substantiates that chain stiffening arises not only from the high segment density around the branched points on polymacromonomers but also from enhanced side chain – side chain or main chain – side chain repulsions. Another finding (in Table IV-5) that B in toluene is larger for F33 than for F15 seems reasonable because one bead for the former polymer must contain a larger number of monomeric units and hence must have a larger volume.

References

1. O. Kratky and G. Porod, *Rec. Trav. Chim.*, **68**, 1106 (1949).
2. H. Yamakawa, *Helical Wormlike Chains in Polymer Solutions*, Springer, Berlin, 1997.
3. H. Yamakawa and W. H. Stockmayer, *J. Chem. Phys.*, **57**, 2843 (1972).
4. J. Shimada and H. Yamakawa, *J. Chem. Phys.*, **85**, 591 (1986).
5. See, for example, Miyaki, Y. Ph.D. Thesis, Osaka University, 1981.
6. F. Abe, Y. Einaga, T. Yoshizaki, and H. Yamakawa, *Macromolecules*, **26**, 1884 (1993).
7. K. Horita, F. Abe, Y. Einaga, and H. Yamakawa, *Macromolecules*, **26**, 5067 (1993).
8. F. Abe, K. Horita, Y. Einaga, and H. Yamakawa, *Macromolecules*, **27**, 725 (1994).
9. M. Kamijo, F. Abe, Y. Einaga, and H. Yamakawa, *Macromolecules*, **28**, 1095 (1995).
10. T. Norisuye, A. Tsuboi, and A. Teramoto, *Polym. J.*, **28**, 357 (1996).
11. C. Domb and A. J. Barrett, *Polymer*, **17**, 179 (1976).

Chapter V Viscosity Behavior in Cyclohexane and Toluene

V. 1 Introduction

In Chapters III and IV, we concluded from light scattering measurements that the main-chain length dependence of z-average mean-square radius of gyration $\langle S^2 \rangle_z$ for the polymacromonomers F15 and F33 in cyclohexane at 34.5°C (the Θ point) and in toluene (a good solvent) is explained quantitatively by the current theories for wormlike chains[1] with or without excluded volume and that the chain stiffness is an increasing function of side chain length and higher in the good solvent by about 1.6 times than in the Θ solvent. The present chapter describes a viscometric study undertaken to see whether intrinsic viscosity ($[\eta]$) data for the polymacromonomers in the two solvents are consistent with these conclusions.

As mentioned in Chapter I, Wintermantel et al.[2] encountered a problem that the available theories for the unperturbed wormlike chain[1] did not give a consistent explanation of $\langle S^2 \rangle_z$ and $[\eta]$ for toluene solutions of a polymacromonomer consisting of the poly (methyl methacrylate) (PMMA) backbone and polystyrene (PS) side chains. Thus checking the applicability of the wormlike chain model to $[\eta]$ of our polymacromonomers is the focus of the work in this chapter.

V. 2 Results

The values of $[\eta]$ and the Huggins constant k' obtained for F15 and F33 samples in cyclohexane at Θ (34.5°C) and in toluene at 15°C are all summarized in Tables V-1 and V-2, along with those of the weight-average

Table V-1. Results from Viscosity Measurements on Polymacromonomer F15 Samples in Cyclohexane at 34.5°C and in Toluene at 15°C

		in Cyclohexane at 34.5°C		in Toluene at 15°C	
Sample	$M_w/10^5$ [a]	$[\eta]/cm^3g^{-1}$	k'	$[\eta]/cm^3g^{-1}$	k'
F15-1	64.7	41.6	0.71	115	0.36
F15-2	40.4	33.5	0.70	85.7	0.35
F15-3	22.5	26.4	0.75	53.9	0.39
F15-4	12.3	19.6	0.78	35.1	0.41
F15-5	8.22	16.2	0.87	26.4	0.46
F15-6	6.09	14.2	0.88	21.5	0.48
F15-7	3.81	11.1	0.95	15.7	0.55
F15-8	2.52	9.19	1.07	11.9	0.61
F15-9	1.75	8.02	1.09	9.81	0.66
F15-10	1.23	6.84	1.17	8.20	0.73
F15-11	0.614	5.68	1.18	6.46	0.86
F15-12	0.474	5.51	1.15	6.09	0.87
F15-13	0.260	5.33	1.13	5.82	0.85
F15-14	0.108	5.60	0.98	6.05	0.77
F15-15	0.0514	5.61	0.82	5.89	0.68

[a] From light scattering in toluene (see Chapter IV)

molecular weight M_w. The molecular weight dependence of $[\eta]$ for the F15 polymer in the two solvents is illustrated in Figure V-1. The data points for the respective solvents are fitted by smooth curves which are almost horizontal up to a molecular weight of 6×10^4 and rise linearly with increasing M_w above 4×10^5. The viscosity exponent in this high M_w region is 0.48 for cyclohexane solutions and 0.72 for toluene solutions.

The viscosity data for the polymacromonomer F33 in the two solvents,

Table V-2. Results from Viscosity Measurements on Polymacromonomer F33 Samples in Cyclohexane at 34.5°C and in Toluene at 15°C

		in Cyclohexane at 34.5°C		in Toluene at 15°C	
Sample	$M_w/10^5$ [a]	$[\eta]/cm^3g^{-1}$	k'	$[\eta]/cm^3g^{-1}$	k'
F33-1	108			119	0.35
F33-2	76.5			91.4	0.35
F33-3	51.7	35.8	0.67	68.1	0.36
F33-4	36.2	28.5	0.71	51.6	0.38
F33-5	28.9	24.8	0.73	42.1	0.40
F33-6	22.0	21.4	0.75	33.5	0.43
F33-7	12.0	15.1	0.83	21.4	0.50
F33-8	8.73	11.5	0.88	17.3	0.53
F33-9	7.90	11.5	0.85	15.5	0.64
F33-10	3.84	8.20	1.04	10.2	0.75
F33-13	1.28	6.75	1.13	8.50	0.75
F33-14	0.543	6.95	1.09	8.66	0.78

[a] From light scattering in toluene (see Chapter IV)

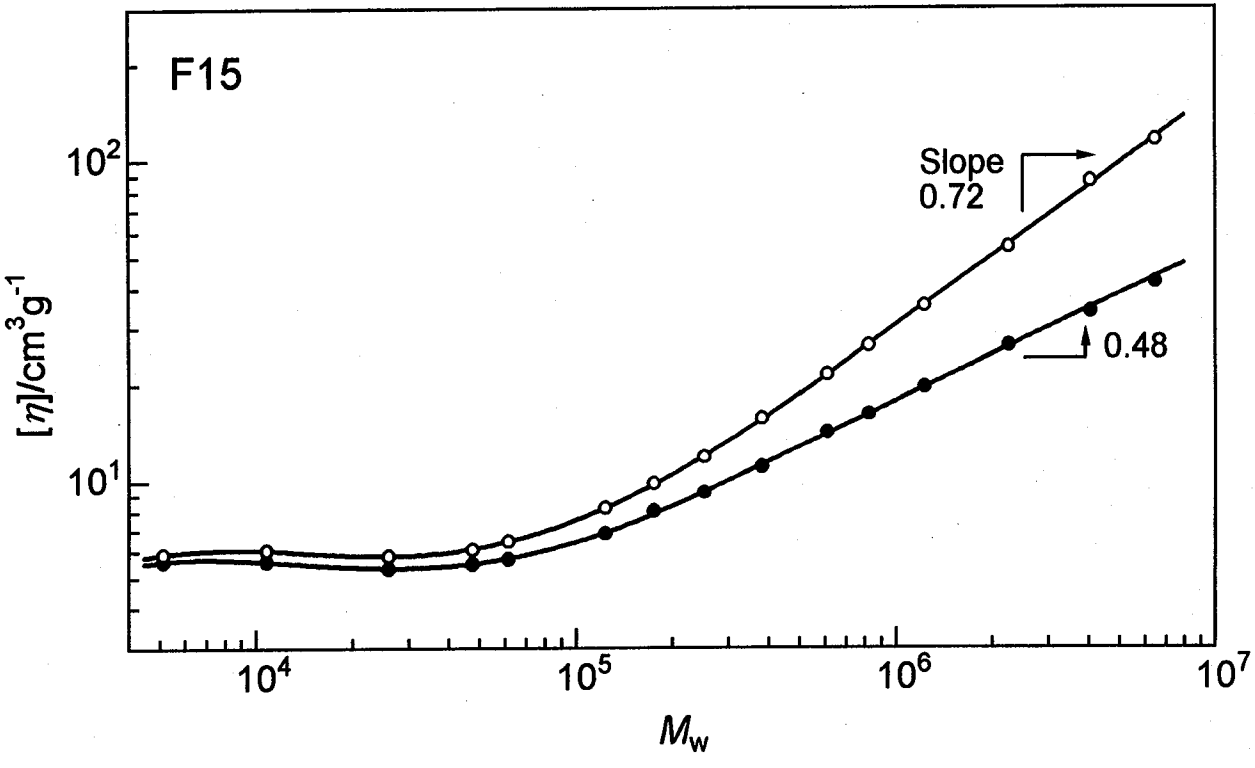

Figure V-1. Molecular weight dependence of $[\eta]$ for the polymacromonomer F15 in cyclohexane at 34.5°C (○) and in toluene at 15°C (●).

displayed in Figure V-2 along with Takeo's data[3] for two samples (the triangles), show similar main-chain length dependence, but the slopes of the curves in the high M_W region, i.e., for $M_W > 8\times10^5$, are larger than those for the F15 polymer in the corresponding solvents, being 0.59 in cyclohexane and 0.79 in toluene. The change in slope from 0 to 0.79 for toluene solutions is similar to what was reported for polymacromonomers consisting of the PMMA backbone and PS side chains in the same solvent at 25°C.[2,4]

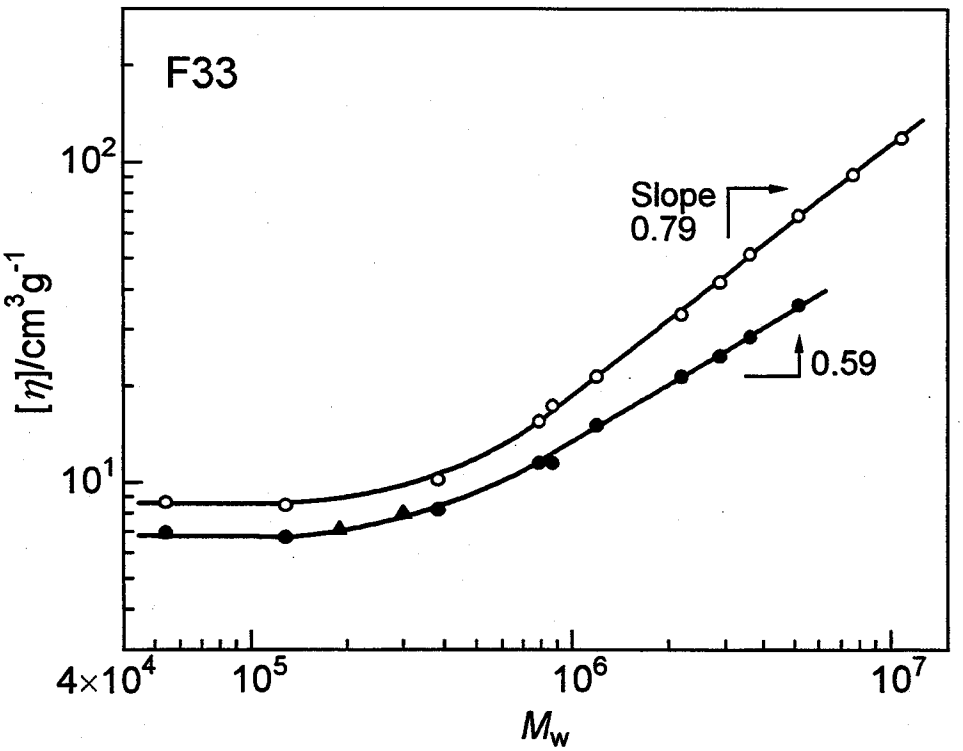

Figure V-2. Molecular weight dependence of $[\eta]$ for the polymacromonomer F33 in cyclohexane at 34.5°C (○) and in toluene at 15°C (●, this work; ▲, Takeo[3]).

V. 3 Discussion

V. 3. 1 Analysis

Data in Cyclohexane at the Θ Point

The intrinsic viscosity $[\eta]_0$ of an unperturbed wormlike chain was formulated by Yamakawa and coworkers[5-8] with the cylinder and touched-bead models. For a given molecular weight M, it is determined by three parameters, the contour length L, the Kuhn segment length λ^{-1}, and the cylinder diameter d or the bead diameter d_b depending on the hydrodynamic model used for the calculation, and the theories based on the two models are essentially equivalent for thin, stiff chains ($\lambda d \lesssim 0.1$) if the difference between d and d_b are taken into account.[8]

For polymacromonomers, the cylinder model[6,7] is probably suitable rather than the touched-bead model,[8] but theoretical $[\eta]_0$ values for short, thick chains with flexibility are available only for the latter model because of the nature of the Kernel in the Kirkwood-Riseman type integral equation.[5-8] Limited theoretical information on the cylinder model (capped with hemispheres at both ends) indicates, however, that the cylinder and touched-bead theories reduce to the Einstein equation for rigid spheres at $L = d = d_b$ and are identical if $L >> d$ and d_b. Furthermore, the difference in $[\eta]_0$ between these theories with $d = d_b$ diminishes with increasing λd and becomes at most $\pm 5\%$ over the entire L range for $\lambda d = 0.2$. Thus we may regard $[\eta]_0$ for the touched-bead chain model[8] with $\lambda d_b \gtrsim 0.2$ as that for the cylinder

model and express the latter as

$$[\eta]_0 = f(\lambda L, \lambda d)/(\lambda^3 M) \qquad \text{(V-1)}$$

where $f(\lambda L, \lambda d)$ is known as a function of λL and λd (= λd_b); though $[\eta]$ in the touched-bead model is given only for the discrete number of beads, we regard that in eq V-1 as a continuous function of L.

With the values of λ^{-1} (9.5 nm for F15 and 22 nm for F33) determined from $\langle S^2 \rangle_z$ in Chapter III, we attempted to estimate a set of M_L (the molar mass per unit contour length) and d which allows eq V-1 to fit the $[\eta]$ data for the polymacromonomer F15 or F33 in cyclohexane at 34.5°C. However, no parameter set explained the very gradual M_w dependence of $[\eta]$ in the low molecular weight region (see Figures V-1 and V-2).

As remarked in Chapter III, some side chains near the main-chain ends may contribute toward apparently increasing L. This end effect is schematically shown in Figure V-3, in which $\delta/2$ stands for the hydrodynamic contribution of side chains to the main-chain contour at each end. With this new parameter, L may be redefined by

$$L = M/M_L + \delta \qquad \text{(V-2)}$$

with M_L being the linear molar mass density in the middle portion of the polymer backbone. In applying eq V-1 with this equation, we assume that both ends of the polymacromonomer are hemispherical. We note that the

end effect on $\langle S^2 \rangle_z$, i.e., the contribution from side chains near the main-chain ends, was insignificant in the molecular weight range studied by light scattering in Chapters III and IV.

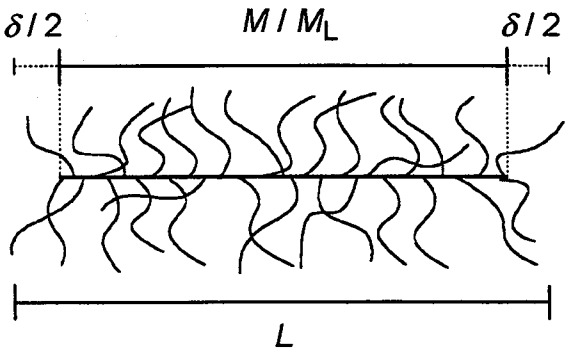

Figure V-3. Schematic representation of the effect of side chains on the contour length of a polymacromonomer.

Again with the λ^{-1} values from $\langle S^2 \rangle_z$, the viscosity data in cyclohexane were analyzed by eq V-1 with eq V-2. The parameters (M_L, d, and δ) thus obtained are summarized in Table V-3, along with the values of λ^{-1} and M_L estimated from $\langle S^2 \rangle_z$, and the theoretical $[\eta]_0$ values (the solid lines) are compared with our data in Figure V-4, in which the left end of each solid curve corresponds to the Einstein sphere limit.[9] It can be seen that the curves closely fit the data points for the respective polymacromonomers down to this limit. The dot-dashed lines in the figure represent the theoretical values for $\delta = 0$. Their deviations from the solid lines become large progressively with decreasing molecular weight below 1×10^6, showing pronounced end effects on $[\eta]$.

In Table V-3, the values of M_L from $[\eta]$ and $\langle S^2 \rangle_z$ for the respective

polymacromonomers are in good agreement with each other. These M_L's with the molecular weights of the macromonomers (1.65×10^3 for F15 and 3.56×10^3 for F33) give h (the monomeric length along the main-chain contour) values of about 0.26 nm that are close to 0.25 nm for the *all-trans* conformation. Thus, we may conclude that the wormlike chain is a good model for the two polymacromonomers in cyclohexane at **Θ**.

Although, as the λ^{-1} values in Table V-3 indicate, the polymacromonomers in cyclohexane are considerably stiff, the viscosity exponents (0.48 for F15 and 0.59 for F33) are unusually small even at high M_w where the end effect is insignificant. According to the $[\eta]_0$ theory based on the cylinder[6,7] or touched-bead[8] model, the viscosity exponent is determined not by λ^{-1} itself but by the magnitude of λd and is smaller for

Table V-3. Wormlike-Chain Parameters for the Polymacromonomers F15 and F33 in Cyclohexane at 34.5°C and in Toluene at 15°C

			M_L	d	δ	λ^{-1}	B
Polymer	Solvent	T/°C	10^3 nm^{-1}	nm	nm	nm	nm
F15	CH [a]	34.5	6.3 (6.2)[c]	4.7	2.2	9.5 [c]	0
F15	Tol [b]	15	6.3	5.0	2.3	16 [c]	4.5 [c]
F33	CH	34.5	13.5 (13.0)[c]	7.4	4.0	22 [c]	0
F33	Tol	15	13.8	8.5	4.3	36 [c]	18 [c]

[a] Cyclohexane

[b] Toluene

[c] Analysis from $\langle S^2\rangle_z$ data (Chapters III and IV)

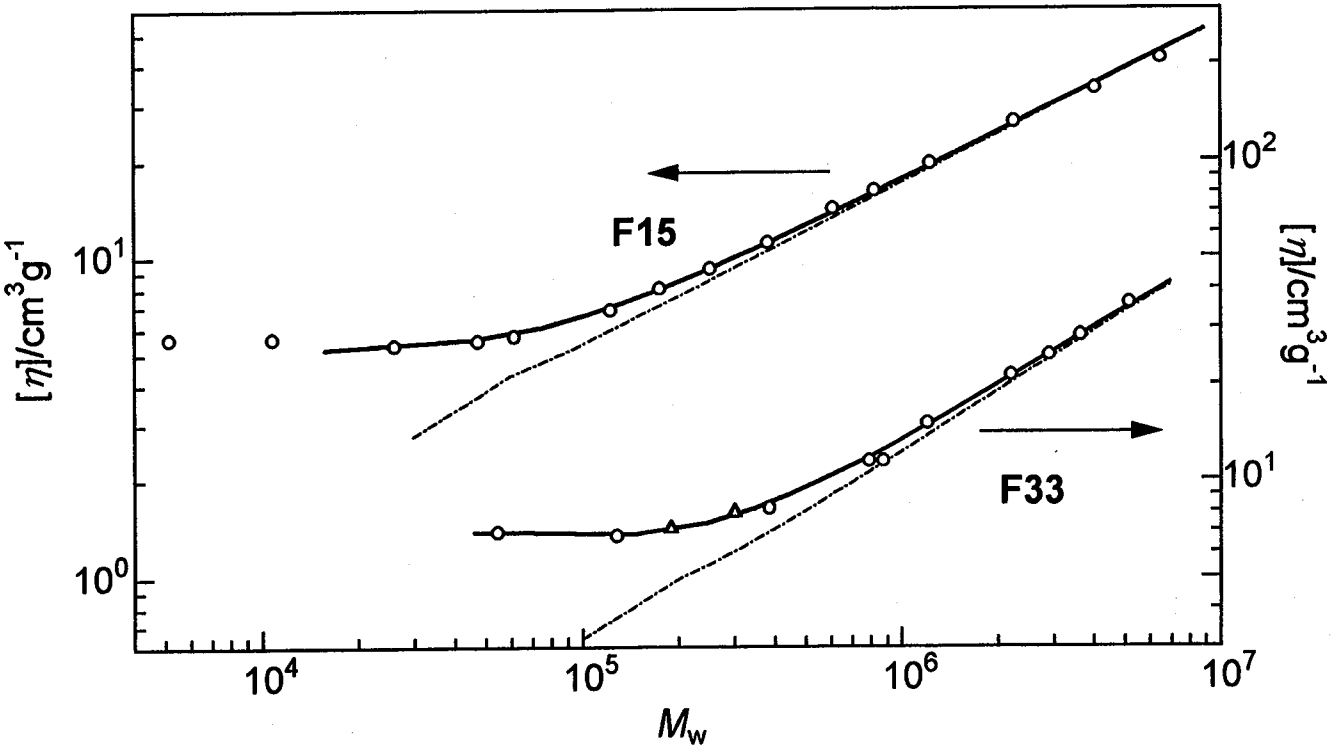

Figure V-4. Comparison between the measured $[\eta]$ (○, this work; △, Takeo[3]) for the polymacromonomers F15 and F33 in cyclohexane at 34.5°C and the theoretical solid curves for the unperturbed wormlike chains with the parameters given in Table V-3. Dot-dashed lines, theoretical values for $\delta = 0$.

larger λd. In fact, the λd values for our polymers F15 and F33 in cyclohexane are 0.49 and 0.33, respectively, being comparable to that for linear PS in the same solvent.[10] Thus, these polymacromonomers in the Θ state exhibit viscosity behavior as if they were flexible.

Data in Toluene

As shown in Chapter IV, excluded volume effects on $\langle S^2 \rangle_z$ for the polymacromonomers F15 and F33 in toluene are significant at high M_w and explained quantitatively by the quasi-two-parameter (QTP) theory[5,11,12] for wormlike[1] or helical wormlike[5] bead chains. Within the framework of this theory, the viscosity-radius expansion factor α_η [$\equiv ([\eta] / [\eta]_0)^{1/3}$] is a universal function of the scaled excluded-volume parameter $\tilde{z}$ defined by eq IV-2 with eqs IV-3 and IV-4.

Adopting the Barrett function[13] for α_η^3, we have

$$\alpha_\eta^3 = \left(1+3.8\tilde{z}+1.9\tilde{z}^2\right)^{0.3} \qquad \text{(V-3)}$$

which reduces to the original Barrett equation in the coil limit where $\tilde{z}$ equals the conventional excluded-volume parameter. Equation V-3 is known to accurately describe experimental data for linear flexible and semiflexible polymers[10,14-18] over a broad range of molecular weight.

Equations IV-2 through IV-4 with eqs V-1 – V-3 indicate that $[\eta]$ in a perturbed state is characterized by five parameters, λ^{-1}, M_L, d, δ, and B (the

excluded-volume strength defined by eq IV-5). A curve fitting procedure was employed for our analysis with λ^{-1} and B fixed to the values determined from $\langle S^2 \rangle_z$ in toluene; we note that more than three parameters could not uniquely be determined from the present $[\eta]$ data. The estimated parameters, together with the assumed values for λ^{-1} and B, are presented in Table V-3.

Figure V-5 shows that the theoretical solid curves calculated with these parameters for the two polymacromonomers closely fit the data points over the entire M range where theoretical values are available. This agreement may be taken to substantiate that the wormlike chain model is applicable to our polymacromonomers in the good solvent, too, since the estimated M_L and hence h for each polymer essentially agree with those from both $\langle S^2 \rangle_z$ and $[\eta]$ in cyclohexane at the Θ temperature. The dashed lines in Figure V-5 refer to the unperturbed state (i.e., $B = 0$). Their downward deviations from the perturbed lines show the significance of excluded volume effects on $[\eta]$ for our polymacromonomers in toluene. Though not shown here, the end effects on $[\eta]$ were remarkable at low M_w as in cyclohexane (see the dot-dashed lines in Figure V-4). Hence, consideration of both excluded-volume and end effects seems almost mandatory in the analysis of $[\eta]$ data for a polymacromonomer covering a broad range of M_w in a good solvent, though the former effect in a stiffer chain is generally less significant. Wintermantel et al.[2] should carefully re-examine $[\eta]$ data for their polymacromonomers in toluene by taking into account these effects.

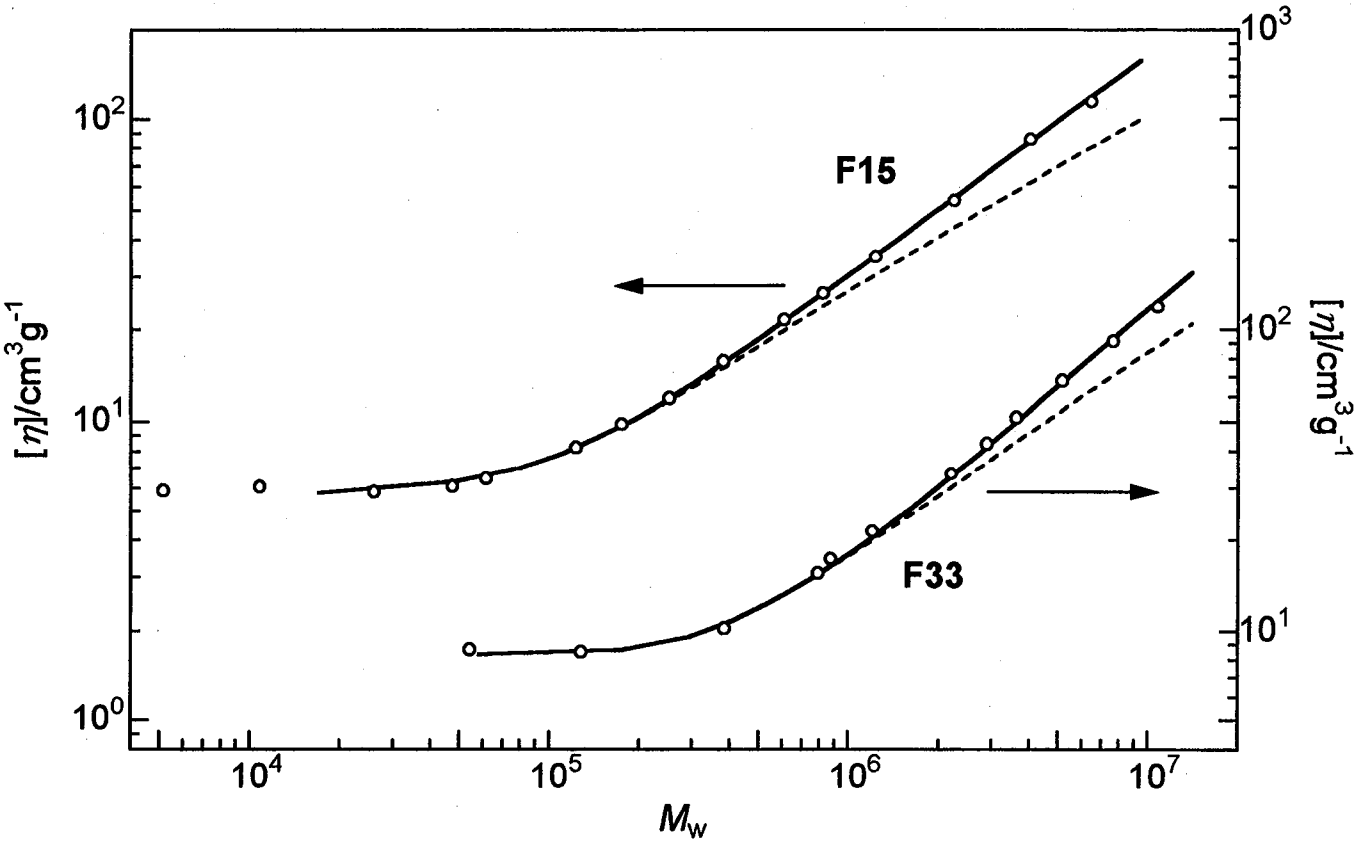

Figure V-5. Comparison between the measured $[\eta]$ (○) for the polymacromonomers F15 and F33 in toluene at 15°C and the theoretical solid curves for the perturbed wormlike chains with the parameters given in Table V-3. Dashed lines, theoretical values for the unperturbed intrinsic viscosity.

V. 3. 2 Viscosity Factor

The circles, filled and unfilled, in Figure V-6 show the values of the Flory viscosity factor Φ [= $[\eta]M_w/(6\langle S^2\rangle_z)^{3/2}$] for our polymacromonomers in cyclohexane at 34.5°C and in toluene at 15°C, respectively, calculated from the data in Tables V-1 and V-2 and the $\langle S^2\rangle_z$ data (see Tables IV-1 – IV-4). A common feature of the data points for the respective polymer + solvent systems is that Φ gradually decreases with increasing M_w, and for both F15 and F33 polymers Φ is systematically larger in the Θ solvent than in the good solvent. These trends resemble those for short flexible chains[5,10,19] rather than long stiff chains.[20]

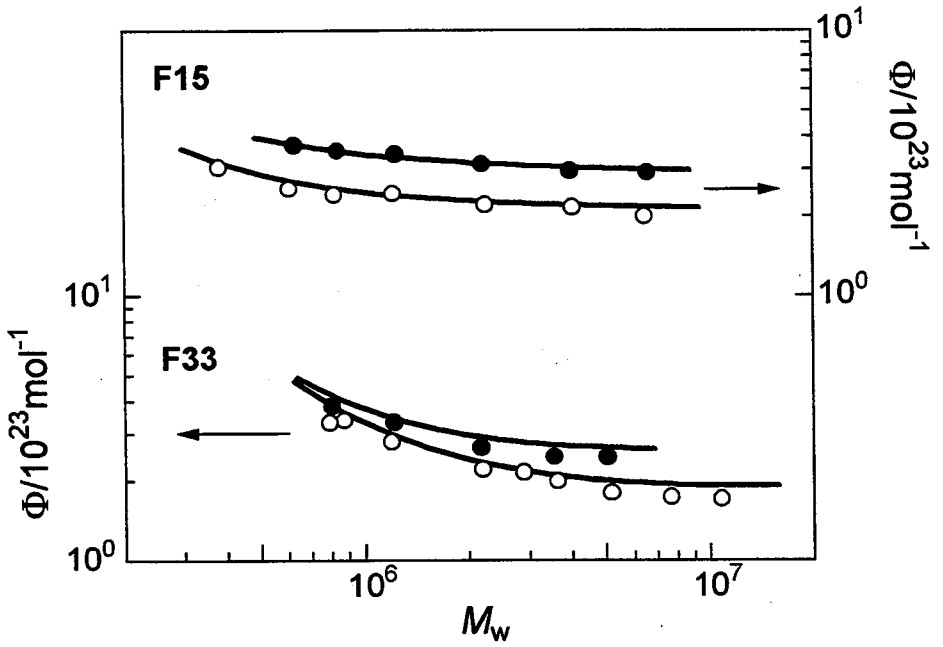

Figure V-6. Experimental Φ for the polymacromonomers F15 and F33 in cyclohexane at 34.5°C (●) and in toluene at 15°C (○) compared with the theoretical curves. See the text for the parameters used.

The curves in Figure V-6 represent the theoretical Φ values for the wormlike chains with the parameters in Table V-3, computed from eqs V-1 – V-3 for $[\eta]$, eq III-1 for the unperturbed mean-square radius of gyration, and eq IV-1 for the radius expansion factor. We note that the means of M_L from $[\eta]$ and $\langle S^2\rangle_z$ (6250 nm^{-1} for F15 and 13400 nm^{-1} for F33) have been used for the calculation and also that, as already mentioned, the end effect on $\langle S^2\rangle_z$ can be neglected in the M_w range concerned here. Though the curves for F33 appear somewhat above the data points because of the small discrepancy between the M_L values from $\langle S^2\rangle_z$ and $[\eta]$, the agreement between theory and experiment is rather satisfactory. This confirms that $\langle S^2\rangle_z$ and $[\eta]$ for our polymacromonomers in both Θ and good solvents are consistently explained by the wormlike chain model.

V. 3. 3 Chain Diameter

As expected, the value of d for the polymacromonomer F33 in cyclohexane or toluene, given in Table V-3, is considerably lager than that for F15, and both are much larger than that known for linear PS in cyclohexane (d = 0.75 nm or d_b = 1.01 nm).[5,10] We suspected that the hydrodynamic diameter for either polymacromonomer in cyclohexane at the Θ temperature is roughly twice as large as the unperturbed root-mean-square end-to-end distance $\langle R^2\rangle_0^{1/2}$ of the linear PS chain with same number of monomer units as each side chain (the side chain molecular weight is 1.53×10^3 for F15 and 3.44×10^3 for F33), and calculated $\langle R^2\rangle_0^{1/2}$ from the known expression[5] for

the unperturbed helical wormlike chain with $\lambda^{-1}\kappa_0$ (the reduced curvature) = 3.0, $\lambda^{-1}\tau_0$ (the reduced torsion) = 6.0, λ^{-1} (the static stiffness parameter) = 2.06 nm, and M_L = 358 nm^{-1}.[21,22] The resulting $\langle R^2\rangle_0^{1/2}$ is 2.4 nm for F15 and 3.8 nm for F33. If the wormlike chain with λ^{-1} = 2.0 nm and M_L = 390 nm^{-1} (see ref. 22) is used, essentially the same $\langle R^2\rangle_0^{1/2}$ values are obtained because of the weak helical nature of the linear PS molecule. These calculated end-to-end distances are in almost perfect agreement with the $d/2$ values for the polymacromonomers in cyclohexane (see Table V-3). Thus eq V-1 with eq V-2 allows us to deduce the shape or structure of the polymacromonomers in the Θ state in not only the longitudinal but also the lateral directions to the backbone.

The estimated d for either polymacromonomer in toluene at 15°C is slightly larger than that in cyclohexane at 34.5°C. This suggests that enhancement of repulsion between neighboring side chains in toluene causes the side chains to extend. As found from $\langle S^2\rangle_z$ in Chapter IV and confirmed indirectly from $[\eta]$ in this chapter, the chain stiffness also increases when the solvent is changed from the Θ to good condition. In short, excluded-volume interactions play an important role in the global conformation or structure of a polymacromonomer in solution.

References and Notes

1. O. Kratky and G. Porod, *Rec. Trav. Chim.*, **68**, 1106 (1949).
2. M. Wintermantel, M. Schmidt, Y. Tsukahara, K. Kajiwara, and S. Kohjiya, *Macromol. Rapid Commun.*, **15**, 279 (1994).
3. Y. Takeo, M.S. Thesis, Osaka University, 1997.
4. Y. Tsukahara, S. Kohjiya, K. Tsutsumi, and Y. Okamoto, *Macromolecules*, **27**, 1662 (1994).
5. H. Yamakawa, *Helical Wormlike Chains in Polymer Solutions*, Springer, Berlin, 1997.
6. H. Yamakawa and M. Fujii, *Macromolecules*, 7, 128 (1974).
7. H. Yamakawa, and T. Yoshizaki, *Macromolecules*, **13**, 633 (1980).
8. T. Yoshizaki, I. Nitta, and H. Yamakawa, *Macromolecules*, **21**, 165 (1988).
9. The values of λd for the polymacromonomers in cyclohexane are not sufficiently small compared to unity, implying that the polymers are not completely rigid even in the sphere limit where $L = d$. However, the present analysis ignores such small flexibility of the two hemispherical caps at the chain ends. Though the values of δ themselves may have no much significance, they are about one half those of d (see Table V-3) and seem reasonable.
10. Y. Einaga, H. Koyama, T. Konishi, and H. Yamakawa, *Macromolecules*, **22**, 3419 (1989).
11. H. Yamakawa and W. H. Stockmayer, *J. Chem. Phys.*, **57**, 2843 (1972).
12. J. Shimada and H. Yamakawa, *J. Chem. Phys.*, **85**, 591 (1986).
13. A. J. Barrett, *Macromolecules* **17**, 1566 (1984).
14. F. Abe, Y. Einaga, and H. Yamakawa, *Macromolecules*, **26**, 1891 (1993).
15. K. Horita, F. Abe, Y. Einaga, and H. Yamakawa, *Macromolecules*, **26**, 5067 (1993).
16. F. Abe, K. Horita, Y. Einaga, and H. Yamakawa, *Macromolecules*, **27**, 725 (1994).
17. M. Kamijo, F. Abe, Y. Einaga, and H. Yamakawa, *Macromolecules*, **28**,

1095 (1995).
18. T. Norisuye, A. Tsuboi, and A. Teramoto, *Polym. J.*, **28**, 357 (1996).
19. K. Akashi, Y. Nakamura, and T. Norisuye, *Polymer*, **39**, 5209 (1998).
20. See, for example, H. Murakami, T. Norisuye, and H. Fujita, *Macromolecules*, **13**, 345 (1980).
21. T. Konishi, T. Yoshizaki, T. Saito, Y. Einaga, and H. Yamakawa, *Macromolecules*, **23**, 290 (1990).
22. T. Konishi, T. Yoshizaki, and H. Yamakawa, *Macromolecules*, **24**, 5614 (1991).
23. T. Norisuye and H. Fujita, *Polym. J.*, **14**, 143 (1982).

Chapter VI Summary and Conclusions

This thesis has been concerned with the conformation and dilute-solution properties of two polymacromonomers (F15 and F33) consisting only of polystyrene with fixed side chain residues of 15 and 33, with the primary interest in exploring the relation between the molecular architecture and chain stiffness of the regular comb polymers in cyclohexane at different temperatures of 32°C – 45°C and in toluene at 15°C. The samples prepared in this work are narrow in molecular weight distribution and cover a very broad range of (total) weight-average molecular weight M_W from 5.1×10^3 – 6.5×10^6 for F15 and from 5.4×10^4 – 1.1×10^7 for F33. The main results and conclusions derived from light scattering and viscosity measurements on these samples are summarized as follows.

Chain Dimensions and Stiffness in Cyclohexane and Toluene (Chapters III and IV)

The two polymacromonomers have solubility features very similar to those of linear polystyrene in that they have a Θ point in cyclohexane at 34.5°C and large, positive second virial coefficients in toluene. The measured z-average radii of gyration $\langle S^2\rangle_z$ for either polymacromonomer in the former solvent exhibited non-Gaussian behavior, thus showing an unmistakable semiflexibility of the polymer backbone. These data were analyzed on the basis of the unperturbed wormlike chain to estimate the Kuhn segment length λ^{-1} and the molar mass M_L per unit contour length. The

contour length per main chain residue obtained for each polymer in the Θ state from the estimated M_L (6200 nm^{-1} for F15 and 13000 nm^{-1} for F33) was close to the value 0.25 nm expected for the *all-trans* conformation of the linear polystyrene molecule, being quite insensitive to the side-chain length. On the other hand, λ^{-1} remarkably increased (from about 2 nm for linear PS to 22 nm for F33) with increasing side chain length. Thus, even in the absence of intramolecular excluded-volume interaction (in the conventional framework), the semiflexibility of polymacromonomers arises from the high segment density around the main chain.

In cyclohexane at temperatures other than the Θ point, excluded-volume effects on $\langle S^2 \rangle_z$ were detected for both polymacromonomers at high M_w, and they were more pronounced in toluene, a good solvent. The $\langle S^2 \rangle_z$ data in these non-ideal solvents were therefore analyzed with the aid of the quasi-two-parameter theory for excluded-volume effects. It was found that as the excluded-volume strength increases in cyclohexane, λ^{-1} gradually increases, and that in toluene, it becomes almost 1.6 times as large as that in the Θ state. We thus arrived at the conclusion that main chain – side chain and side chain – side chain repulsions are also responsible for the semiflexibility of polymacromonomers.

Viscosity Behavior (Chapter V)

Intrinsic viscosity ($[\eta]$) data for the polymacromonomers in cyclohexane at 34.5°C and in toluene at 15°C (a good solvent) were similarly analyzed, but the analysis ended up with finding disagreement between theory and

experiment for M_W below 10^6. This failure was attributable to the end effect arising from side chains near the main-chain ends. In fact, when the effect was taken into consideration, the current theories for wormlike chains with or without excluded-volume effect were found to explain the $[\eta]$ data almost quantitatively. The estimated parameters were consistent with those determined from $\langle S^2 \rangle_z$, confirming the conclusion from light scattering that for the polymacromonomers F15 and F33 the chain stiffness is higher in the good solvent than in the Θ solvent, while the monomeric length along the backbone contour is close to that expected for the *all-trans* conformation in both solvents. Thus, our important conclusion is that the wormlike chain model is applicable to $\langle S^2 \rangle_z$ and $[\eta]$ for the two polymacromonomers in both Θ and good solvents.

The hydrodynamic diameter estimated from $[\eta]$ for each polymer in cyclohexane was about twice as large as the unperturbed root-mean-square end-to-end distance of the linear polystyrene chain with the same number of monomer units as each side chain in the polymacromonomer. The diameter in toluene is slightly larger than that in cyclohexane, indicating that repulsions between neighboring side chains cause not only the backbone stiffness but also the average side chain length to increase.

List of Publications

Part of this thesis has been or will be published in the following papers.

1. Polymacromonomer Consisting of Polystyrene: Light Scattering Characterization in Cyclohexane.
   Ken Terao, Yoshishige Takeo, Masataka Tazaki, Yo Nakamura, and Takashi Norisuye, *Polym. J.*, **31**, 193 – 198 (1999).

2. Solution Properties of Polymacromonomers Consisting of Polystyrene.
   2. Chain Dimensions and Stiffness in Cyclohexane and Toluene.
   Ken Terao, Yo Nakamura, and Takashi Norisuye, *Macromolecules*, **32** (1999), in press.

3. Solution Properties of Polymacromonomers Consisting of Polystyrene.
   3. Viscosity Behavior in Cyclohexane and Toluene.
   Ken Terao, Toshio Hokajo, Yo Nakamura, and Takashi Norisuye, Submitted to *Macromolecules*.

4. Solution Properties of Polymacromonomers Consisting of Polystyrene.
   Ken Terao, Yo Nakamura, and Takashi Norisuye, in *Molecular Interactions and Time-Space Organization in Macromolecular Systems*, Y. Morishima, T. Norisuye, and K. Tashiro eds., Springer, Berlin, in press.

Other related papers

1. Excluded-Volume Effects in Star Polymer Solutions: Four-Arm Star Polystyrene in Cyclohexane near the Θ Temperature.
   Mitsuhiro Okumoto, Ken Terao, Yo Nakamura, Takashi Norisuye, and Akio Teramoto, *Macromolecules*, **30**, 7493 – 7499 (1997).

2. Light-Scattering and Phase-Separation Studies on Cyclohexane Solutions of Four-Arm Star Polystyrene.

   Ken Terao, Mitsuhiro Okumoto, Yo Nakamura, Takashi Norisuye, and Akio Teramoto, *Macromolecules*, **31**, 6885 – 6890 (1998).

3. Liquid Crystallinity of Concentrated Solutions of Polymacromonomers Consisting of Polystyrene.

   Koji Maeno, Yo Nakamura, Ken Terao, Takahiro Sato, and Takashi Norisuye, *Kobunshi Ronbunshu*, in press.